Università di Foggia

PhD thesis in Basic and Clinical Neuroscience
XXXVIII° cycle

Parkin mutant iPSC-derived dopaminergic neurons display altered circadian clock-dependent mitochondrial energy metabolism and dynamics

TUTOR
Prof. Nazzareno Capitanio

PhD CANDIDATE
Mirko Tamma

NAZZARENO
CAPITANIO
11.12.2025
12:54:18
GMT+01:00

Academic year 2024/2025

INDEX

1 ABSTRACT

Mutations in genes related to mitochondrial quality control, like PARK2, have been associated with almost half of the autosomal recessive forms of early onset Parkinson's disease (PD). The PARK2 gene encodes for Parkin, an E3 ubiquitin ligase involved in mitophagy-mediated removal of damaged mitochondria. Recent studies have highlighted a link between mitochondrial function and the cell's molecular circadian clock.

The aim of this study was to investigate the interplay between mitochondrial bioenergetics, mitochondrial dynamics, and the cell-autonomous circadian clock in iPSC-derived dopaminergic neurons from PD patients carrying PARK2 mutation. We demonstrated that *in vitro*-synchronized control neurons exhibited robust autonomous oscillations of mitochondrial oxidative phosphorylation (OxPhos) and of mitochondrial network dynamics. By contrast, neurons carrying the Parkin mutation displayed a pronounced dampening of these oscillations. Morphological analysis showed that control neurons cyclically shifted between interconnected and fragmented mitochondrial network states, whereas Parkin-mutant neurons remained persistently fragmented. Transcriptional profiling indicated dysregulation of fusion–fission and mitophagy regulators, with DRP1 and PINK1 upregulated in PD neurons. Notably, analysis of the core clock genes revealed deregulated expression patterns in PD derived dopaminergic neurons.

These findings support a reciprocal interplay between the circadian clock gene machinery and mitochondrial function, suggest a Parkin-mediated regulatory mechanism, and unveil a previously underappreciated layer of complexity in Parkinson's disease pathophysiology that may contribute to dopaminergic neurons vulnerability.

2 INTRODUCTION

2.1 Parkinson's disease

Parkinson's disease (PD) was first described in 1817 by James Parkinson as "shaking palsy". Around 50 years later, the neurologist Jean Martin Charcot conducted in-depth studies of the condition and renamed it "maladie de Parkinson" (Parkinson's disease).[1,2] It is the second most common chronic neurodegenerative disease after Alzheimer's. Its global incidence ranges from 5 to over 35 new cases per 100,000 people per year, and it is estimated that it affects 0.3% of the population. This number increases sharply with age, affecting over 3% of people over 80.[2]

Individuals affected by the condition present with clinical symptoms that are generally categorised as motor and non-motor.[3] Motor symptoms include bradykinesia, muscle rigidity, tremors and postural instability[4]; while non-motor symptoms include olfactory dysfunction, cognitive impairment, psychiatric symptoms, sleep disturbances and autonomic dysfunction.[5] Several studies have suggested that non-motor symptoms appear much earlier than motor symptoms, which supports the idea that they can be used to diagnose the condition in its early stages.

Neuropathology

The neuropathology of PD is characterised by the selective loss of dopaminergic neurons in the *substantia nigra pars compacta* (SNpc), a nucleus of neural cells located in the midbrain and forming part of the extrapyramidal system. (**Figure 1**). From a physiological perspective, they are the primary producers of dopamine, a neurotransmitter that activates and regulates the movement control circuit.

At the histological level, intracytoplasmic protein aggregates termed Lewy bodies are observed; these are primarily composed of α-synuclein and, to a lesser extent, ubiquitin, neurofilaments and molecular chaperones. The

presence of Lewy bodies is not exclusive to PD; indeed, they have been detected not only in dopaminergic neurons but also in other neurodegenerative diseases. The presence of Lewy bodies alone constitutes a pathology termed Lewy body disease, which initially occurs in the cholinergic and monoaminergic neurons of the brainstem and in the neurons of the olfactory system, but also spreads to the limbic and neocortical regions as the disease progresses.[2]

In the typical case, the onset of symptoms occurs when 50–80% of the dopaminergic neurons in the SNpc are no longer functioning. Widespread neurodegeneration is then generally observed throughout the central nervous system.[6] The pathology is the result of multiple levels of cellular dysfunction, including mitochondrial and lysosomal dysfunction, alterations in calcium and α-synuclein homeostasis, neuroinflammation, and oxidative stress.

At present, treatment of the disease is based primarily on pharmacological replacement of dopamine (L-DOPA), but non-dopaminergic approaches and deep brain stimulation techniques are also used for patients who develop motor complications caused by L-DOPA treatment.[2]

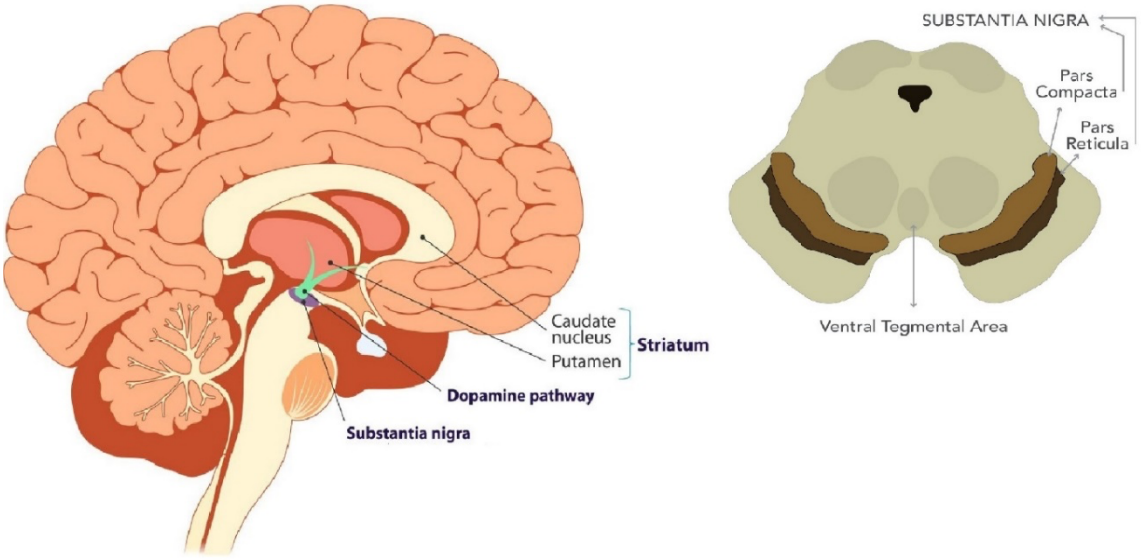

Figure 1: Location of the *substantia nigra pars compacta* (SNpc)

Etiology

Despite extensive research, the etiology of PD remains elusive, with the identification of two predominant forms: one familial and the other sporadic, or idiopathic. The manifestation of symptoms can occur at any age; however, it is considered unusual if they appear before the age of 40 and is regarded as extremely rare if they appear before the age of 20. The latter cases are generally attributable to familial hereditary forms.[7]

The loss of SNpc neurons, which is concomitant with the onset of symptoms, has been associated with genetic, environmental and immunological factors.

Genetic factors pertain to alterations in proteins implicated in the maintenance of neural cell homeostasis, and their prevalence has been predominantly observed in familial forms of PD, accounting for approximately 10% of all documented cases.[8,9]

The prevailing opinion among researchers is that environmental factors are principally associated with sporadic forms of PD. However, the extant literature suggests that these factors can both increase and reduce the risk of developing the disease. Several factors have been identified as being associated with a reduced risk, including the consumption of tobacco products, coffee, non-steroidal anti-inflammatory drugs, calcium channel blockers and alcohol. The following factors have been identified as increasing the risk of disease: exposure to pesticides, head injuries, rural living, use of β-blockers, agricultural occupation, and consumption of well water.[10]

Recently, the possible involvement of the immune system, particularly autoimmune mechanisms, in the etiopathogenesis of PD has also been hypothesised.[11] Neuroinflammation is generally considered a hallmark of the disease; however, the prevailing view is that its role in either promoting or protecting against neurodegeneration remains to be fully elucidated. Conventionally, the notion was that the disease did not involve such mechanisms; nevertheless, accumulating evidence from the preceding decade

on immune alterations has reinforced this association.[12] A substantial increase in the levels of innate immune components was observed in the substantia nigra and cerebrospinal fluid, including cytokines and complement[13]; furthermore, increases in γδ+ T cells in both peripheral blood and cerebrospinal fluid were documented.[14]

Considering this plurality of causative factors, PD is regarded as a multifactorial disease, in which genetic, environmental and immunological factors may act either individually or in combination with each other. This results in the identification of two distinct clinical conditions: a classic form that exhibits all the primary symptoms of PD, and an atypical form. The atypical condition is characterised by the presence of symptoms including bradykinesia, multisystem atrophy, progressive supranuclear palsy and corticobasal degeneration.

2.2 Genetic factors

Over the past two decades, significant advances have been made in the identification of the genetic basis of PD, particularly with regard to monogenic causes of the disease.[1] While 15% of PD patients have a family history, and 5–10% suffer from a monogenic form of the disease with Mendelian inheritance, the majority of cases are sporadic with unknown etiology.[15]

Initially, research into the genetics of PD focused on rare familial forms of the disease. However, following numerous gene association studies, a series of gene variants involved in the pathogenesis or protection against the disease have been discovered.[15,16] The most significant developments in this field have been achieved through the introduction of GWAS (Genome Wide Association Study) and the integration of novel technologies, including NGS (Next Generation Sequencing) and exome sequencing.[17,18]

Several of the proteins transcribed by PD-associated genes are involved in multiple molecular pathways. Alterations to these pathways can generate neuropathology that is indistinguishable from the sporadic form. Genome-

wide association studies (GWAS) have confirmed that certain genes are altered in sporadic forms of PD. Examples of these pathways include: α-synuclein proteostasis, mitochondrial function, oxidative stress, calcium homeostasis, axonal transport and neuroinflammation.[2]

To date, at least 23 loci and 19 genes have been identified as being causative of PD (**Table 1**): these include 10 autosomal dominant genes, 9 autosomal recessive genes and several genetic risk loci and variants associated with sporadic PD.[1] However, the relevance of some of these genes and variants remains unclear due to a lack of replication studies and functional validation.[19]

Loci	Gene	Protein	Inheritance	Onset	References
PARK1	*SNCA*	α-synuclein	AD	early	[20]
PARK2	*PRKN*	parkin RBR E3 ubiquitin protein ligase	AR	early	[21]
PARK3	*Unknown*		AD	late	[22]
PARK4	*SNCA*	α-synuclein	AD	early	[23]
PARK5	*UCHL1*	ubiquitin C-terminal hydrolase L1	AD	early / late	[24]
PARK6	*PINK1*	PTEN induced putative kinase 1	AR	early	[25]
PARK7	*DJ-1*	parkinsonism associated deglycase	AR	early	[26]
PARK8	*LRRK2*	leucine rich repeat kinase 2	AD	late	[27]
PARK9	*ATP13A2*	ATPase 13A2	AR	early	[28]
PARK10	*Unknown*		Risk factor	late	[29]
PARK11	*GIGYF2*	GRB10 interacting GYF protein 2	AD	late	[30]
PARK12	*Unknown*		X-linked	late	[31]
PARK13	*HTRA2*	HtrA serine peptidase 2	AD	early / late *	[32]
PARK14	*PLA2G6*	phospholipase A2 group VI	AR	early	[33]
PARK15	*FBXO7*	F-box protein 7	AR	early	[34]
PARK16	*Unknown*		Risk factor	late	[35]
PARK17	*VPS35*	vacuolar protein sorting 35	AD	late	[36]
PARK18	*EIF4G1*	eukaryotic translation initiation factor 4 gamma 1	AD	late	[37]

PARK19	*DNAJC6*	DnaJ Hsp40 member C6	AR	early	38
PARK20	*SYNJ1*	synaptojanin 1	AR	early	39,40
PARK21	*TMEM230*	transmembrane protein 230	AD	early / late *	41
	DNAJC13	DnaJ Hsp40 member C13	AD	early / late *	42
PARK22	*CHCHD2*	coiled-coil-helix-coiled-coil-helix domain containing 2	AD	early / late *	43
PARK23	*VPS13C*	vacuolar protein sorting 13 homolog C	AR	early	44
	RIC3	RIC3 acetylcholine receptor chaperone	AD	early / late*	45

Table 1: loci and genes involved in the etiopathogenesis of PD

AD: Autosomal Dominant, AR: Autosomal Recessive, *: few cases studied

Parkin RBR E3 ubiquitin protein ligase

In 1997, a locus on chromosome 6q25.2-q27 (PARK2) was identified that was associated with a form of autosomal recessive juvenile parkinsonism (ARJP).[46] Subsequent research by Kitada et al. (2013) revealed that this form of the disease is caused by an exon deletion in the PRKN gene.[21] To date, at least 268 variants of this gene have been documented, and it is the most prevalent cause of juvenile parkinsonism.[1]

ARJP is a severe form of PD with an onset that frequently occurs before the age of 20. Patients present with L-DOPA-responsive parkinsonism, L-DOPA-induced dyskinesia and motor fluctuations. On a pathological level, there is loss of neurons in the *substantia nigra* and *locus ceruleus*, and absence of Lewy bodies.[21,46]

PRKN is 1.380 kb long, contains 12 exons, and encodes a protein called parkin consisting of 465 amino acids. Parkin is a type of E3 ubiquitin ligase called an RBR (RING-in-between-RING) and consists of a ubiquitin-like domain (UBL) at the N-terminal end and four zinc-coordinating RING domains: RING0, RING1, IBR (in-between RING) and RING2.[47]

At a physiological level, Parkin is primarily expressed in the brain, where it plays a role in the selective degradation of misfolded or damaged proteins, as well as in the regulation of mitochondrial homeostasis. As an E3 ubiquitin ligase, Parkin works alongside E1 ubiquitin-activating and E2 ubiquitin-conjugating enzymes within the ubiquitin-proteasome system (UPS) to break down specific target proteins. Typically, E3 enzymes control substrate recognition and regulate ubiquitination activity.[1] The UBL domain interacts with the RING1 domain to negatively regulate ligase activity, translocation to mitochondria, and parkin-dependent mitophagy.[48]

PRKN mutations can cause E3 ubiquitin ligase dysfunction, which compromises mitochondrial homeostasis and the degradation of target proteins in the SUP, resulting in the accumulation of potentially neurotoxic proteins, especially in the *substantia nigra*.[15]

Prkn$^{-/-}$ models of *Drosophila melanogaster* manifest classic Parkinsonian symptoms, including degeneration of dopaminergic neurons, motor dysfunction, mitochondrial dysfunction, infertility and a reduced lifespan[49]; In contrast, Prkn$^{-/-}$ mouse models exhibit mitochondrial dysfunction and striatonigral deficits, but do not show loss of dopaminergic neurons.[50] A genetic study in Drosophila has demonstrated that VPS35, an additional PD-causing gene, interacts with parkin, and that the over-expression of VPS35 can balance the effects of parkin dysfunction.[51]

2.3 Mitochondrial dysfunction

Mitochondria are the organelles responsible for producing energy in cells. They consist of two phospholipid membranes and form a complex, highly dynamic network that is regulated by fusion and fission. Their other important functions include signalling pathways, cell proliferation, intracellular calcium regulation and apoptosis control. Although they have their own genome consisting of a double-stranded circular DNA molecule measuring 16.6 kb, this only codes for some subunits of respiratory chain complexes. Most

mitochondrial proteins are encoded by the nuclear genome and require the coordinated processes of transcription, translation, translocation and assembly of complexes within the mitochondria.[52]

The ability of mitochondria to produce energy is closely related to their number and shape. The number of mitochondria in a given cell type reflects its metabolic needs and can vary greatly between different types of cells. In order to respond effectively to changes in energy demand, cells require an efficient system of both mitochondrial biogenesis and mitophagy. The balance between these two processes determines the mitochondrial content of the cell. PGC-1α and PGC-1β are key proteins in mitochondrial biogenesis, while PINK1, Parkin and BNIP3 are responsible for mitophagy.[53]

The size and morphology of mitochondria play an important role in energy production. They can exist as small, individual organelles or as extensive tubular networks, which result from the fusion of multiple mitochondria. These elongated, fused mitochondria exhibit higher mitochondrial respiration and are found in cells with high energy demands, as well as during energy-consuming processes. The main proteins involved in mitochondrial fusion are mitofusin (MFN) 1 and 2 and optic atrophy 1 (OPA1), while those responsible for mitochondrial fission are dynamin-related protein 1 (DRP1) and fission 1 (FIS1). The interactions between mitochondrial fusion and fission are known as "mitochondrial dynamics".[53,54] Furthermore, mitochondrial morphology can vary dramatically between cell types and tissues, representing a response to metabolic signals from cells and their environment.[55] Mitochondria can form extensive networks through the process of fusion, and conversely become highly fragmented through fission. It is hypothesised that the process of fusion enables the exchange of material between healthy mitochondria, while fission facilitates the separation of intact and damaged mitochondria.[56]

Dysfunctions in the regulation, function and dynamics of mitochondria can cause damage, especially in tissues with high energy demands, such as the

brain, muscles, heart, kidneys and liver. The neurological symptoms associated with this type of dysfunction include developmental delays, cognitive decline, seizures, blindness and loss of motor skills.[52]

Studies have confirmed that mitochondrial dysfunction is associated with several age-related diseases, and that damaged mitochondria accumulate as we age. This age-related accumulation is a significant risk factor for a number of neurodegenerative diseases, including PD.[57] The characteristic symptoms of PD result from the degeneration of dopaminergic neurons in the SNpc and subsequent dopamine depletion. These neurons are highly sensitive to mitochondrial dysfunction due to their high metabolic activity, which leads to the production of a greater number of reactive oxygen species (ROS). These ROS can subsequently damage the mitochondria. If these ROS are not adequately removed, they can spread their harmful effects throughout the entire mitochondrial network, ultimately causing cell death.[58]

The initial hypothesis proposing a link between PD and mitochondrial dysfunction emerged following the observation that exposure to MPTP (a molecule present in synthetic heroin) resulted in the onset of parkinsonism and degeneration of dopaminergic neurons, via the inhibition of Complex I. This inhibition leads to a reduction in mitochondrial ATP production and an increase in reactive nitrogen species and ROS, consequently inducing elevated oxidative stress. Subsequent studies revealed that reduced Complex I activity was also present in various tissues of patients with sporadic PD, including skeletal muscle and platelets.[59]

This association was further confirmed by the discovery of PINK1 and parkin. Mutations in these proteins are the most common cause of early-onset recessive PD, and both cause degeneration of dopaminergic neurons. Parkin and PINK1 cooperate in the removal of damaged mitochondria through mitophagy, and alteration of either leads to the accumulation of non-functioning mitochondria, resulting in cell death.

2.4 Parkin

Parkin structure

Parkin is a 465 amino acid-long RBR (RING in-between RING) E3 ubiquitin ligase containing a ubiquitin-like domain (UBL) at the N-terminal end and the RBR structure at the C-terminal end, formed by four zinc-coordinating RING-like domains: RING0, RING1, IBR (between RINGs) and RING2, and between the IBR and RING2 domains there is a REP (repressor element of parkin) domain (**Figure 3**).

The UBL domain is implicated in substrate recognition, association with the proteasome, and regulation of cellular levels and activity of parkin.[47] The protein has a compact structure that is stabilised by multiple hydrophobic interactions. The UBL domain uses its hydrophobic surface to bind to the RING1 domain, while the C-terminal catalytic domain is associated with the RING0 domain. The RING0 and RING2 domains each coordinate two zinc ions through histidine and cysteine residues.[60] The presence of zinc ions is essential for structural stability and the regulation of enzyme activity. RING0 binds zinc ions in a hairpin configuration that is unique to parkin, whereas IBR and RING2 exhibit a sequential arrangement of residues. RING1 coordinates zinc ions using a cross-brace arrangement that is common to other E3 ligases and represents the binding site for E2 proteins. (**Figure 2**).[47]

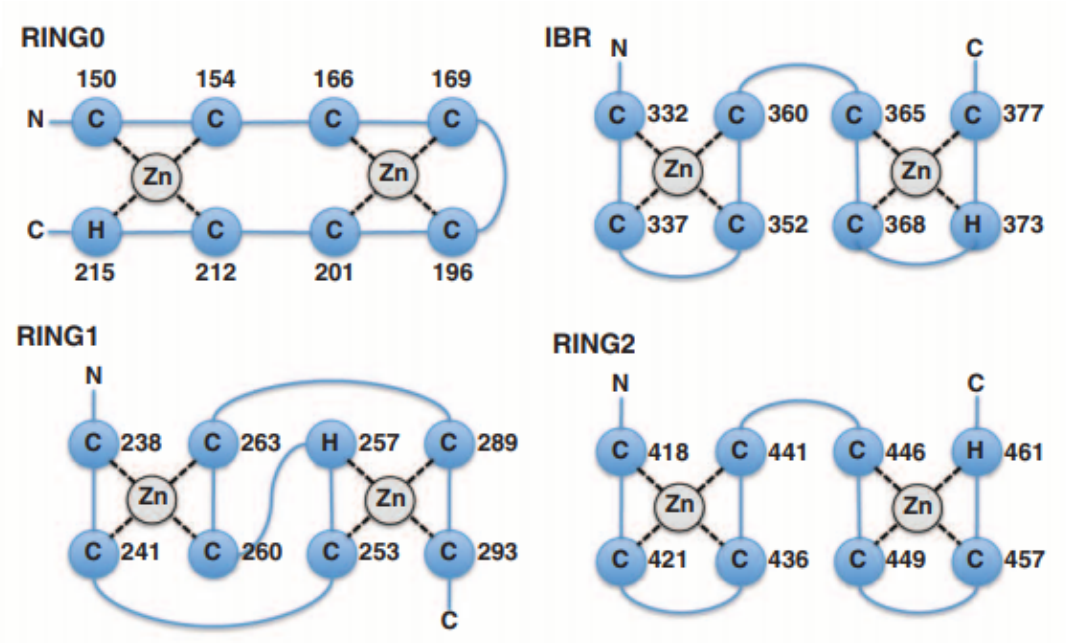

Figure 2: Topology of zinc-ion–coordinating domains[61]

The RING2 domain contains the catalytic site and the catalytic cysteine (Cys431), which accepts ubiquitin from the E2 enzyme and transfers it to the substrate. The IBR domain is conserved among members of the RBR E3 family, but its precise function remains unclear. Parkin also contains two flexible interdomain linkers. The first consists of a sequence of 70 poorly conserved residues that follow the UBL domain. The second is located between the IBR and RING2 domains. It is composed of disordered segments and an alpha-helix that binds the RING1 domain. This helix is called the repressor element of parkin (REP) due to its role in regulating Parkin activity. RING0 is a unique parkin domain and, as with the IBR domain, its exact function is not yet known.

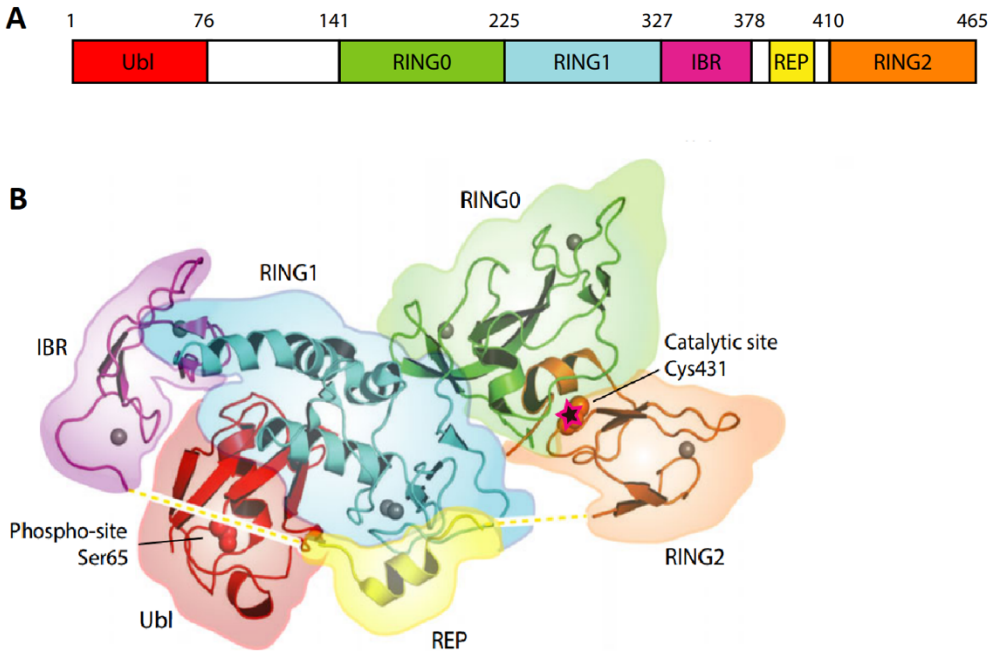

Figure 3: Parkin structure[47]

A) Scheme of parkin domains. B) Representation of the protein structure. The grey spheres indicate the zinc ions present in the structure.

Ubiquitination

Ubiquitination is a post-translational modification that marks proteins for degradation by the proteasome or lysosomes. The elimination of proteins or organelles that do not function properly due to specific damage or a physiological ageing process is the basis of cellular homeostasis. The process of marking is initiated by the addition of ubiquitin monomers and chains to lysine residues or N-terminal groups of the substrate protein. This process is catalysed by three types of enzymes, which act sequentially: E1 ubiquitin-activating enzymes, E2 ubiquitin-conjugating enzymes and E3 ubiquitin ligases (**Figure 4 A**).

E1 hydrolyses an ATP molecule to activate a ubiquitin molecule and conjugate it, through the formation of a thioester bond, between its catalytic cysteine and the C-terminal carboxyl group of ubiquitin. The ubiquitin is then transferred to a second cysteine of an E2 enzyme, making this enzyme "loaded".

The loaded E2 enzyme interacts with a specific E3 enzyme and transfers ubiquitin to the amino groups of the target protein. Throughout the process, the E3 ubiquitin ligase enzyme provides specificity, regulation in substrate recognition and control of activity.[62] Ubiquitin contains seven lysine residues and an N-terminal amino group, which are used to form different types of polyubiquitin chains. The two most common types of chain are K48 and K63. In these chains, multiple ubiquitin molecules are linked in a linear arrangement, with the C-terminus of one molecule attached to lysine 48 or 63 of the next molecule. Each chain type corresponds to a particular signal for degradation.

E3 enzymes fall into three distinct classes depending on their structure and chemical mechanisms: RING-type, HECT-type and RING-HECT hybrids (**Figure 4 B**). E3 RING-type enzymes are distinguished by the presence of a C3HC4-type RING domain that binds the E2 enzyme but does not participate directly in the reaction. This class of E3 functions as an inert scaffold to facilitate the direct transfer of ubiquitin from E2 to the substrate.[47]

E3 HECT-type enzymes contain a HECT domain (homologous to the E6-AP C-terminus) with a cysteine residue at the active site. This residue accepts ubiquitin from an E2 enzyme via a thioester intermediate and transfers it to the substrate.

Enzymes in the third class, known as RING-HECT hybrids, form the RBR family of E3 ubiquitin ligases, combining the chemical properties of HECT-type enzymes with the structural properties of RING-type enzymes. RBRs contain a C3HC4-type RING domain (RING1), followed by two zinc-binding Cys/His-rich domains (IBR and RING2). The RING2 domain contains an active site with a cysteine residue that accepts ubiquitin from the E2 enzyme and transfers it to the substrate.[63]

Parkin belongs to the RBR E3 ubiquitin ligase family and can ubiquitinate a variety of proteins, including itself and outer mitochondrial membrane proteins, in response to mitochondrial depolarisation.

Accumulation of polyubiquitin chains on mitochondria triggers the recruitment of autophagosomes and proteasomes, initiating the mitophagy process. Parkin can form different types of ubiquitin chains, primarily K63, K48, K11 and K6, and exhibits relatively flexible substrate specificity.[64] Its activity is strictly regulated and usually suppressed, but it can be activated by various conditions, such as mitochondrial depolarisation or the activation of the epidermal growth factor signalling pathway.[65]

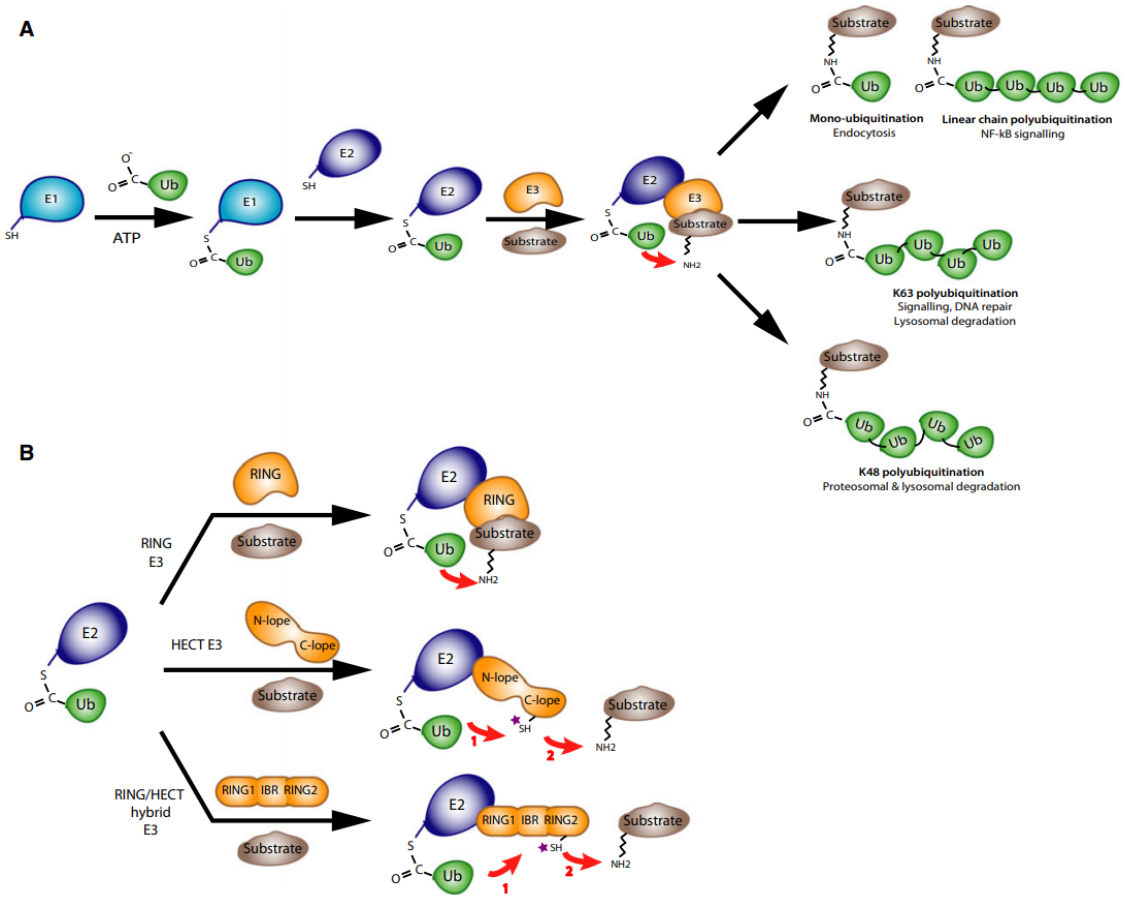

Figure 4: Ubiquitination[47]

A) Cascade of enzymes involved in the ubiquitination process and types of ubiquitin chains. B) Class of E3 ubiquitin ligase enzymes and mechanism of action.

Self-inhibition and activation of parkin

Parkin is controlled by several mechanisms that limit its activity. The first mechanism involves the blocking of the RING2 catalytic domain by the RING0 domain. The second mechanism involves the control of the binding site

with the E2 enzyme present on the RING1 domain, which is normally blocked by the UBL and REP domains. Finally, the large distance between the E2 binding site and the catalytic site on RING2 stops ubiquitin from being transferred from the E2 enzyme to the catalytic cysteine of parkin. Several in vitro studies have provided insight into some of the molecules that can activate parkin and the mechanisms underlying this process. The UBL domain plays an important role in parkin activation, as some of the molecules that interact with this domain are associated with parkin activation.[66] The UBL domain binds its substrates using the same hydrophobic surface that it uses to interact with the RING1 domain. This indicates that the UBL and RING1 domains must dissociate upon activation.

PINK1 has been found to activate parkin. It acts upstream of parkin and is necessary for its activation and recruitment to depolarised mitochondria. PINK1 can phosphorylate the UBL domain of Parkin on the serine 65residue (Ser65), or a ubiquitin molecule on the same residue. In turn, phosphorylated ubiquitin molecules can activate parkin by increasing the rate of ubiquitin transfer from the E2 enzyme.[67] Parkin exhibits a higher binding affinity for phospho-ubiquitin, and its phosphorylation at the Ser65 residue increases this affinity by approximately 20-fold. In cells, the expression of non-phosphorylatable ubiquitin delays the recruitment of Parkin to depolarised mitochondria. Mutation of both Ser65 residues in Parkin and ubiquitin suppresses Parkin activation.[68] PINK1 can also phosphorylate ubiquitin in polyubiquitin chains, making them more resistant to the action of deubiquitinases.

While the structural details behind Parkin activation remain unknown, most evidence suggests a simple two-state system: activation triggers a “butterfly” movement, whereby the protein folds along the axis between the RING0 and RING1 domains, bringing the two active sites closer together.[69]

The parkin phosphorylation site is located near the REP linker in the autoinhibited conformation, where it may promote the displacement of the UBL domain and the REP linker, thereby enabling binding with E2 enzymes.

2.5 The role of Parkin in the mitochondrial quality control system

PINK1/Parkin pathway

PINK1 is a mitochondrial damage sensor that can trigger repair or removal mechanisms for damaged mitochondrial elements. In the absence of harmful stimuli, PINK1 is imported into the mitochondrial matrix via the TOM and TIM complexes. Once in the matrix, it is cleaved by the mitochondrial protease MPP and the inner membrane protease PARL. The resulting processed PINK1 is then released into the cytoplasm, where it is degraded by the proteasome. This process results in relatively low endogenous levels of PINK1 in the presence of healthy mitochondria (**Figure 5 A**). Within the mitochondria, PINK1 has also been implicated in the phosphorylation of certain inner mitochondrial membrane proteins, which is believed to play a protective role. Among the proteins phosphorylated by PINK1 are the protease HTRA2/Omi (PARK13), the chaperone TRAP1, and the NDUFA10 subunit of Complex I.[52]

The import of PINK1 and other proteins into mitochondria requires an active proton gradient. The absence of this gradient causes PINK1 to accumulate on the outer mitochondrial membrane, where it becomes stabilised by autophosphorylation and formation of a multimeric complex with TOM. The dissipation of the proton gradient occurs in damaged mitochondria or can be experimentally induced by uncoupling agents such as CCCP (carbonyl cyanide m-chlorophenyl hydrazone) or valinomycin. Once stabilised on the outer mitochondrial membrane, PINK1 is positioned with its kinase domain facing the cytoplasm. It has been hypothesised that PINK1 may interact with cytosolic

and mitochondrial proteins to modulate mitochondrial dynamics and apoptotic signalling. PINK1 can phosphorylate Parkin at the Ser65 residue to activate its enzymatic function and induce its translocation to damaged mitochondria. This process has been confirmed experimentally by treating cell cultures with an uncoupling agent. Within a few hours of treatment with CCCP, Parkin is selectively recruited to damaged mitochondria, which are then removed.[47] The phosphorylation of Parkin causes its autoinhibited structure to be released, leading to enzymatic activation.

PINK1 also phosphorylates ubiquitin and polyubiquitin chains. Phospho-ubiquitin acts as a receptor for Parkin; its binding to the RING1 domain causes a conformational change leading to the initial release of the autoinhibitory UBL domain. This, in turn, facilitates the phosphorylation of parkin, which causes further structural rearrangements, activates enzymatic activity and maintains an active conformation.[70] The combination of PINK1-mediated phosphorylations fully activates Parkin's enzymatic functions.[52]

The recruitment of Parkin to damaged mitochondria initiates a feedforward cycle: activated Parkin further conjugates ubiquitin molecules to outer mitochondrial membrane proteins and thus provides more ubiquitin substrates for PINK1-mediated phosphorylation, which in turn amplifies activation, recruitment, and E3 ligase activity.[67] The consequence of this process is the accumulation of phospho-ubiquitin chains on the surface of damaged mitochondria (**Figure 5 B**).

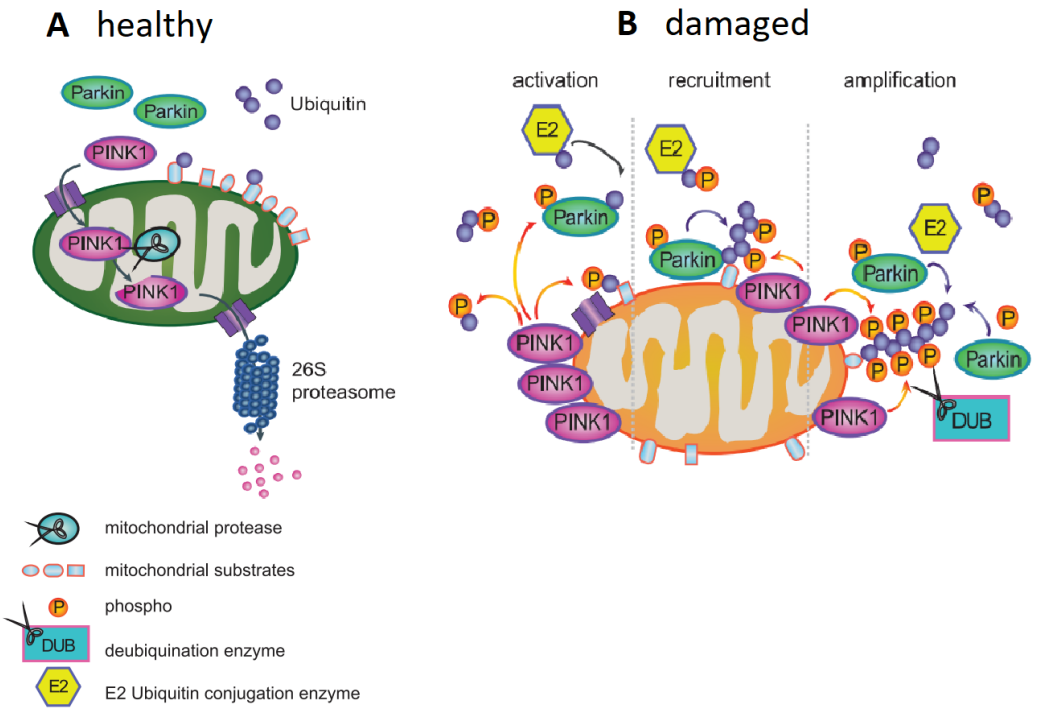

Figure 5: pathway PINK1/Parkin[52]

A) In healthy mitochondria, PINK1 is imported and cleaved by mitochondrial proteases. It is then exported to the proteasome where it is degraded. Parkin remains inactive in the cytoplasm. B) In damaged mitochondria, PINK1 accumulates on the outer mitochondrial membrane and recruits Parkin. PINK1 and Parkin initiate a feedforward amplification cycle. Deubiquitinating enzymes can cleave polyubiquitin chains to reverse the action of PINK1/Parkin.

Mitochondrial quality control directed by PINK1/Parkin

The PINK1/Parkin pathway is a complex, regulated, sequential process that coordinates various aspects of mitochondrial quality control, depending on the extent of damage to the mitochondria. To achieve this, Parkin and PINK1 interact with a wide range of substrate proteins, mediating their clearance.

The pathway's most studied and characterised function concerns the activation of the mitophagy process: the accumulation of phospho-ubiquitin on the surface of mitochondria acts as a mitophagic signal, leading to the recruitment of autophagic receptors.[52] Five ubiquitin-binding proteins, including OPTN (Optineurin), NDP52 (nuclear dot protein 52), p62/SQSTM1, NBR1 (neighbour of BRCA1 gene 1) and TAX1BP1 (Tax1-binding protein 1), bind to polyubiquitin chains and LC3 (microtubule-associated proteins 1A/1B

light chain 3)/GABAARAP (GABAA receptor-associated protein) proteins.[71] The attachment of the autophagosome membrane is mediated by the LC3 interacting region, which tags damaged mitochondria for clearance by the lysosome (**Figure 6**).[72]

The PINK1/Parkin pathway interacts with the mitochondrial fusion proteins Mitofusin 1 and Mitofusin 2. These proteins are marked for degradation to prevent damaged mitochondria from fusing with healthy elements of the network. Mitofusins are eliminated by the valosin-containing protein (VCP/p97) via the 26S proteasome in a process known as mitochondrial-associated degradation (MAD) (**Figure 6**).[73] This process promotes the fragmentation of damaged mitochondria, facilitating their subsequent absorption by autophagosomes.

Other substrates involved in mitochondrial dynamics include the Miro 1 and Miro 2 proteins, which anchor mitochondria to microtubules via the motor protein kinesin, playing a role in mitochondrial trafficking. Degradation of these transporter proteins inhibits mitochondrial movement and further promotes the segregation of damaged mitochondria.[52]

Recent studies have revealed that the PINK1/parkin pathway plays a part in forming so-called mitochondrial-derived vesicles (MDVs), which seem to provide an alternative degradation pathway (**Figure 6**). Mass spectrometry studies in *Drosophila* have shown slower turnover of mitochondrial respiratory chain proteins in PINK1$^{-/-}$ and parkin$^{-/-}$ mutants compared to Atg7$^{-/-}$ autophagy mutant flies.[74] Although this suggested a mechanism of mitochondrial protein turnover that was dependent on PINK1 and parkin, but independent of autophagy, it was subsequently shown that mitochondrial components were degraded via an MDV system. MDVs transport oxidised proteins and lipids to peroxisomes or lysosomes in a process involving multi-vesicular bodies.[75–77] It should be noted that some of these MDVs are generated by VPS35 (PARK17), a component of the retromer complex involved in protein sorting that has also been localised to mitochondria.

While many other proteins from all mitochondrial compartments have been identified as targets of PINK1 and Parkin, their additional functional roles beyond mere elimination remain unclear.[52] Recently, several types of polyubiquitin chain have been identified on substrates, which suggests that the elimination process is subject to more complex regulation mediated by topological differences in polyubiquitin chains.[78]

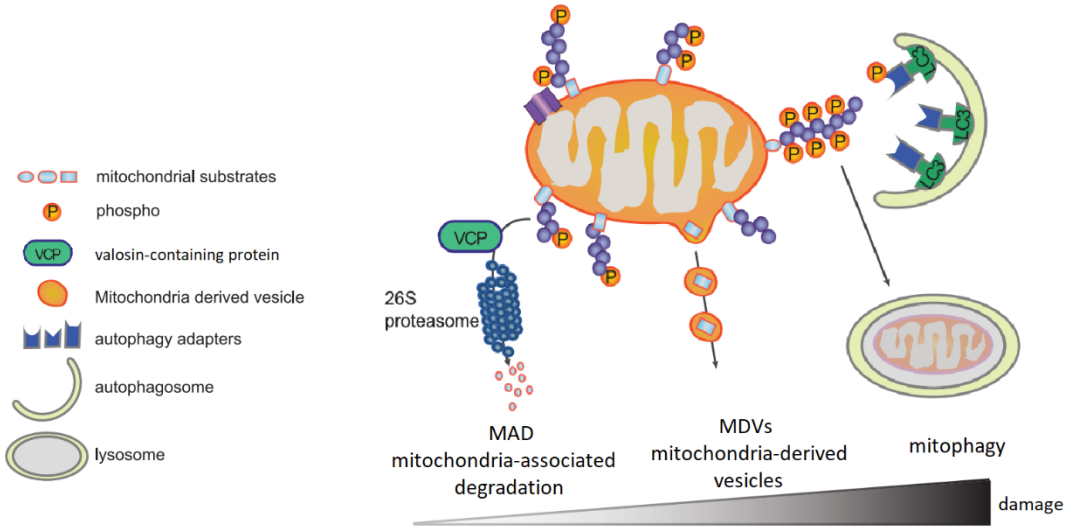

Figure 6: mitochondrial clearance[52]

MAD: Individual proteins marked with ubiquitin can be extracted from the membrane and degraded by the proteasome. MDV: Major localised damage is removed via the formation of vesicles. Mitophagy: when mitochondria are severely damaged, multiple phospho-ubiquitin chains mark them for recognition by autophagic receptors, leading to their degradation in lysosomes.

Mitochondria and cell death

In addition to degrading individual components or entire mitochondria, Parkin also plays a role in mitochondrial biogenesis to balance its degradative functions. *In vitro* studies have demonstrated that, even in the presence of low basal activity, Parkin can ubiquitinate the transcriptional repressor PARIS and direct it towards the proteasome. PARIS degradation promotes the expression of PGC-1α, a key transcriptional regulator of mitochondrial biogenesis.[79] Clearly, the absence of Parkin can compromise the biogenesis, homeostasis and degradation of mitochondria, ultimately resulting in cell death. Parkin protects

cells from a variety of harmful stimuli, making them more resistant when overexpressed and more sensitive when eliminated.

Following stress, Parkin has been shown to prevent the pro-apoptotic protein Bax from translocating into mitochondria, probably by directly ubiquitinating it.[80] Consequently, Parkin inhibits the release of cytochrome c into the cytoplasm and the subsequent induction of apoptosis. Depending on the stress factor, Parkin-mediated induction of mitochondrial quality control and inhibition of Bax-dependent apoptosis may work together to prevent cell death.[52]

2.6 Circadian clock, mitochondrial metabolism and Parkinson's disease

The circadian clock is a complex mechanism that has evolved in all light-sensitive organisms to rhythmically regulate the majority of physiological and behavioral processes. It is an autonomous timing system that governs periods of activity (wakefulness) and rest (sleep), as well as the associated metabolic functions. The term “circadian” derives from the fact that this regulatory system operates in cycles of approximately 24 hours. Circadian regulation operates at multiple levels, ranging from the control of cellular metabolism and the coordination of organs in maintaining blood nutrient homeostasis, to the regulation of sleep–wake cycles in the brain.[81] However, the circadian system does not solely exert rhythmic control over metabolic processes; metabolic signals, in turn, provide an important feedback mechanism to the circadian clock. In essence, metabolism is not merely a downstream consequence of circadian regulation but also plays a key role in modulating the clock itself. This bidirectional feedback system is essential for endowing the circadian clock with the flexibility required to adapt physiological functions to the metabolic demands of cells, tissues, and the entire organism.[82] This system allows the organism to implement a preventive strategy characterized by temporally

programmed responses to environmental stimuli whose rhythmic recurrence stems from their intrinsic periodicity, primarily driven by the solar cycle.

The molecular clock

The molecular mechanisms underlying circadian rhythms are present in all fully differentiated cells. Circadian clocks are organized in a hierarchical manner and consist of different types of clocks with distinct functions within the mammalian circadian system.[82] The molecular oscillator is driven by a transcriptional–translational feedback loop composed of clock genes, such as Period (PER) and Cryptochrome (CRY), which are activated by circadian transcriptional activators, including locomotor output cycles kaput (CLOCK), neuronal PAS domain protein 2 (NPAS2), and aryl hydrocarbon receptor nuclear translocator-like protein 1 (BMAL1).

The core clock mechanism functions as follows: CLOCK–BMAL1 and NPAS2–BMAL1 form heterodimers that bind to E-box elements in the promoter regions of the PER and CRY genes, thereby activating their transcription. The PER and CRY proteins subsequently translocate into the nucleus, where they inhibit the activity of these heterodimers by repressing their own transcription. When PER and CRY levels decline below a certain threshold, the heterodimers regain activity and the cycle restarts. A secondary feedback loop provides additional stability to the oscillatory system. It involves nuclear receptor subfamily 1 group D (REV-ERBα) and RAR-related orphan receptors (ROR), which are activated by components of the core clock. These factors regulate the rhythmic expression of BMAL1 by binding to ROR response elements in its promoter region (**Figure 7**). These intricate feedback loops generate cycles of approximately 24 hours and are therefore defined as circadian. Clock components also form complexes with specific epigenetic regulators to orchestrate the rhythmic expression of target genes outside the core clock mechanism, referred to as clock-controlled genes. These clocks, generally termed “peripheral clocks,” impart circadian rhythmicity to a variety

of tissue-specific functions, including detoxification in the gastrointestinal tract, urine production in the kidneys, and regulation of heart rate.[82]

All peripheral clocks are regulated by the master clock in the brain, which employs the same molecular mechanism composed of clock genes to generate rhythms and coordinate the activity of all clocks. Comprising 10,000–20,000 neurons, the master clock is located in the suprachiasmatic nucleus (SCN) of the hypothalamus. It is synchronized with external time cues via light, which is detected by melanopsin-containing retinal ganglion cells and transmitted through the retinohypothalamic tract.[83] Neurons of the SCN convey diurnal information to all other clocks in the body via various communication pathways, including endocrine and neuronal routes. These signals also synchronize neighboring hypothalamic regions that regulate a wide range of behavioral and autonomic functions. By orchestrating these pleiotropic regulatory axes, the SCN exerts influence over all organs and cells in the body.[84] However, cellular clocks are also capable of generating rhythmicity in most metabolic functions independently of systemic signals produced elsewhere in the body.

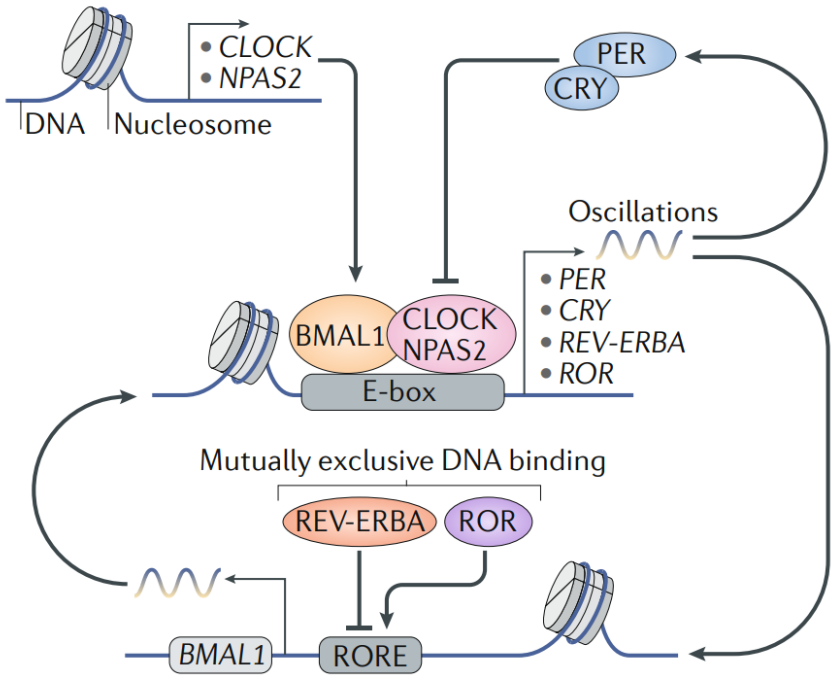

Figure 7: molecular clock mechanism[82]

The CLOCK-BMAL1 and NPAS2-BMAL1 heterodimers activate transcription of the PER, CRY, REV-ERBA and ROR genes. PER and CRY proteins then repress this transcription. Meanwhile, REV-ERBA and ROR proteins drive rhythmic transcription of BMAL1 via ROR response elements (RORE) in the promoter region.

Circadian control of mitochondria

Recent studies have revealed the existence of daily rhythms in mitochondrial content, dynamics, and functions, including respiration and ATP production, highlighting a strong interplay between the circadian clock and mitochondrial metabolism. The oxygen consumption rate (OCR) of whole cells or isolated mitochondria was employed to assess respiration and mitochondrial nutrient utilization and was compared between wild-type mice and mice deficient in clock genes under various experimental conditions.

Mitochondria isolated from the livers of Bmal1 knockout mice, as well as Per1 and Per2 double knockout mice, exhibited lower OCRs compared to their wild-type counterparts.[85,86] Similarly, hepatocytes isolated from mice exhibit an increased respiratory rate during the dark phase compared to the light phase, a phenomenon that is dependent on Bmal1.[87] Furthermore,

mitochondria from liver-specific Bmal1 knockout mice are larger and more rounded, maintaining a consistent morphology throughout the day, whereas wild-type mitochondria exhibit cyclical morphological changes between day and night.[87] Given that fission and fusion regulate mitochondrial function and that respiration is less efficient in fragmented mitochondria, the altered morphology observed in the mitochondria of Bmal1 knockout animals supports the functional changes reported in mitochondrial respiration.[55] These cycles of fission and fusion, and consequently the rhythms of energy production, are regulated by dynamin-related protein 1 (DRP1), a key mediator of mitochondrial fission. DRP1 activity is induced by phosphorylation, which occurs in a circadian manner to coordinate the fragmentation of the mitochondrial network. Inhibition of mitochondrial fission abolishes circadian ATP production and impacts the central circadian clock, thereby affecting overall circadian rhythmicity.[88] Further evidence that mitochondrial function is regulated by the circadian clock comes from experiments on synchronized muscle cells in culture, which display cyclical changes in OCR over a period of approximately 24 hours.[86]

It has also been shown that both the type of diet and the timing of food intake regulate mitochondrial respiration rhythms, with each factor differentially affecting the oscillations of mitochondrial enzymes and the corresponding utilization of substrates.[85]

Parkinson's disease and circadian clock

Recently, imbalances in the circadian system have increasingly been recognized as playing a key role in the onset of PD symptoms, particularly non-motor manifestations. Several studies have reported that motor activity and responsiveness to PD medications vary across the day, in the same way sleep–wake cycles, visual performance, and autonomic function similarly exhibit diurnal fluctuations. Additionally, the patterns of endocrine hormone secretion are also altered. Collectively, these findings suggest that circadian system function and regulation are disrupted in PD.[89] Growing evidence indicates that

reciprocal interactions exist between the dopaminergic system and the circadian rhythm.

On one hand, circadian genes can modulate dopamine synthesis: tyrosine hydroxylase (TH), the rate-limiting enzyme in dopamine production, is regulated by CLOCK. CLOCK influences TH transcription, dopamine transporter activity, and D1 receptor expression by interacting with E-box elements in the promoter regions of these dopamine-related genes.[90] Furthermore, circadian genes may also modulate dopaminergic activity in the ventral tegmental area at the post-transcriptional level.[91]

On the other hand, dopamine is thought to regulate certain clock genes in a receptor-dependent manner. Specifically, dopamine can enhance the transcriptional activity of the CLOCK–BMAL1 complex by promoting the recruitment and phosphorylation of the cAMP-responsive element-binding protein (CREB) transcriptional coactivator.[92] It has been observed that PER2 expression in the dorsal striatum can be modulated by dopamine D2 receptor activation, whereas the PER2 rhythm in the SCN remains unchanged. Consistently, D2 receptor agonists suppress the expression of CLOCK and PER1 genes, while D1 receptor agonists enhance the expression of PER1, CLOCK, NPAS2, and BMAL1.[89] Dopamine also resets circadian rhythms in the SCN during the prenatal stage and, via its receptor-mediated signaling pathways, can regulate melatonin secretion from the pineal gland, which in turn acts as a stimulator of the fetal SCN.[89] In general, alterations in circadian rhythms have been observed in both genetic and induced animal models of PD, as well as in affected patients.[93] In general, alterations in circadian rhythms have been observed in both genetic and induced animal models of PD, as well as in affected patients. Consequently, it is reasonable to associate the fluctuations of symptoms in PD patients with circadian rhythm dysregulation. Furthermore, evidence of these alterations in parkinsonian fibroblasts makes these cells a suitable model for studying the interplay between mitochondrial function and circadian pathways.[93]

In summary, PD results in the loss of dopaminergic neurons and decreased dopamine levels, which in turn disrupt the functioning of circadian clocks, further exacerbating the mitochondrial metabolic dysfunctions already associated with the disease.

3 AIMS

Circadian rhythms are self-regulating mechanisms present in the body, capable of activating or inhibiting most cellular functions in a cyclical manner throughout the day. These rhythms are orchestrated by so-called “molecular clocks,” and it has been demonstrated that mitochondrial functions are also subject to this type of regulation. Specifically, both mitochondrial dynamics and bioenergetic functions undergo circadian oscillations driven by clock genes. Notably, clock genes not only directly regulate mitochondrial functions, but mitochondrial activity, or dysfunction, can also feedback to influence the molecular clock.

Parkinson's disease (PD) is a chronic neurodegenerative disorder characterized by the selective loss of dopaminergic neurons. Nearly half of autosomal recessive forms of juvenile parkinsonism have been linked to mutations in the PARK2 gene, which encodes Parkin, an RBR E3 ubiquitin ligase involved in mitophagy and mitochondrial quality control. Alterations in parkin lead to the accumulation of damaged mitochondria and disruption of cellular bioenergetic processes, ultimately resulting in cell death.

In light of the above considerations, the aims of this study are to:

1. Differentiate induced pluripotent stem cells (iPSCs) derived from healthy fibroblasts and from PD patients carrying PARK2 mutations into neuronal progenitor cells (NPCs) and subsequently into dopaminergic neurons. Differentiation will be assessed through gene expression analysis and immunohistochemistry of the main markers of these cells.
2. Assess the interaction between mitochondrial metabolism and the cellular circadian clock by measuring mitochondrial respiration and glycolytic activity in synchronized iPSC-derived dopaminergic neurons.

3. Investigate the effects of altered mitochondrial quality control on mitochondrial dynamics by labelling mitochondria and monitoring temporal changes in their morphology.

4 MATERIALS AND METHODS

4.1 Cell culture

Skin fibroblasts

Primary skin fibroblasts were obtained from a patient with early-onset PD carrying a heterozygous parkin mutation (del exon 2–3/del exon 3)[93] and from healthy control subjects via punch skin biopsy, following the acquisition of informed consent.

The cells were cultured in DMEM high-glucose (25 mM) enriched with 10% (v/v) fetal bovine serum (FBS), 2 mM L-glutamine, and 1% (v/v) penicillin-streptomycin at 37°C in a humidified atmosphere with 5% CO_2. Cell cultures were typically used at a passage number of less than 10–12 and at a confluence of 80–85%.

iPSCs (induced Pluripotent stem cells)

The iPSCs were obtained in collaboration with the CSS Mendel Institute (Rome, Italy). They were generated through the dedifferentiation of fibroblasts derived from the PD patient and healthy control, following the protocol described by Rosati et al.[94]

Briefly, 1×10^5 skin fibroblasts were nucleofected with three episomal plasmids: pCXLE-hUL (Addgene #27080), pCXLE-hSK (Addgene #27078) and pCXLE-hOCT4-shp53 (Addgene #27077) and plated in fibroblast medium for one week. From day 8 the cells were cultured in mTESR medium (STEMCELL Technologies Inc., Vancouver, BC, Canada). iPSC colonies were manually cut and passaged for expansion. Absence of mycoplasma contamination was verified by PCR analysis using EZ-PCR kit (Biological Industries, Kibbutz Beit Haemek, Israel).

4.2 Matrigel and PLO/Laminin coating

Matrigel® Matrix was purchased from Corning (New York, NY, USA). A 1:40 Matrigel solution in DMEM/F-12 was prepared for coating. The Matrigel solution was poured into the culture medium until the entire surface was covered and left for 1 hour at room temperature. The plate was then washed twice with DMEM/F-12. The plates were heated to 37 °C before use.

Poly-L-Ornithine (PLO) and Laminin were purchased from Sigma-Aldrich (St. Louis, Missouri, USA). The PLO was diluted in PBS to a concentration of 15 µg/mL and poured into the cell culture dishes. After 2 hours of incubation at 37°C, the plates were washed once with PBS and once with DMEM/F-12. Next, a solution of 10 µg/mL laminin in DMEM/F-12 was prepared and poured into the dishes. After 2 hours of incubation at 37°C, the dishes were ready for use.

4.3 iNPCs differentiation

Differentiation was performed using the STEMdiff™ Neural Induction Medium (#05835) and Neural Progenitor Medium (#05833) kits (STEMCELL Technologies Inc., Vancouver, BC, Canada), following the manufacturer's protocol.

iPSCs were dissociated and seeded into AggreWell™800 plates (STEMCELL Technologies Inc., Vancouver, BC, Canada) in Induction Medium to enable embryoid body formation. The plates were incubated for 5 days at 37 °C in a humidified atmosphere with 5% CO_2, with daily medium changes using pre-warmed Induction Medium (37 °C).

On day 5 of differentiation, the embryoid bodies were collected and transferred to Matrigel-coated plates in Induction Medium. The plates were incubated for an additional 6 days under the same conditions, with daily medium replacement.

On day 12, neural rosettes were selected using the Neural Rosette Selection Reagent (STEMCELL Technologies Inc., Vancouver, BC, Canada) and transferred to Matrigel-coated plates in Induction Medium. The cultures were incubated for an additional 5 days at 37 °C in a humidified atmosphere with 5% CO_2, with daily medium changes using pre-warmed Induction Medium.

On day 18, the cells were dissociated using Accutase™ and reseeded onto Matrigel-coated plates in Progenitor Medium. The cultures were maintained at 37 °C and 5% CO_2, with daily replacement of Progenitor Medium. Differentiation efficiency was subsequently evaluated by immunocytochemical analysis.

4.4 Dopaminergic neurons differentiation

iNPCs were differentiated into midbrain dopaminergic neurons using the STEMdiff Midbrain Neuron Differentiation (#100-0038) and the STEMdiff Midbrain Neuron Maturation (#100-0041) Kits (STEMCELL Technologies Inc., Vancouver, BC, Canada) according to the manufacturer's instructions.

The iNPCs were detached with Accutase™ and seeded in PLO/Laminin-coated plates at a density of 90,000 cells/cm² in Progenitor Medium. The next day, the medium was changed to Differentiation medium supplemented with human recombinant shh (#78065, STEMCELL Technologies Inc.). The medium was replaced daily for six days. On day seven, the cells were detached with Accutase™ and reseeded in PLO/Laminin-coated supports at a density of 60,000 cells/cm² in Maturation medium. A half medium change was performed every three days with Maturation medium. Neurons were tested after 25-30 days of maturation. Differentiation efficiency was evaluated through gene expression analysis of specific neuronal markers and confirmed by immunocytochemical characterization.

4.5 Immunocytochemical analysis

For the immunocytochemical analysis of iNPCs, the STEMdiff™ Human Neural Progenitor Antibody Panel (#69001; STEMCELL Technologies Inc., Vancouver, BC, Canada) was used, which includes antibodies against Nestin, PAX6, OCT4 and SOX1. The working dilutions were: Nestin 1:1000, PAX6 1:200, OCT4 1:500 and SOX1 1:500.

For the evaluation of neuronal differentiation, a mouse anti-TH antibody (1:1000; #60058, STEMCELL) and a rabbit anti-MAP2 antibody (1:1000; #5622, Sigma-Aldrich) were employed. As secondary antibodies, anti-mouse or anti-rabbit IgGs conjugated to Alexa Fluor 488 or Alexa Fluor 647 (1:500; Thermo Fisher Scientific, Waltham, MA, USA) were used.

The cells were seeded on different supports coated with Matrigel or PLO/Laminin, fixed with 4% paraformaldehyde for 30 minutes, and permeabilized with 0.1% Triton X-100 in PBS for 20 minutes. A blocking buffer (0.1% Triton X-100, 5% BSA, 5% FBS, 0.02% NaN_3 in PBS) was applied for 10 minutes at room temperature. Primary and secondary antibodies were diluted in a solution containing 0.1% Triton X-100, 0.5% BSA, 5% FBS, and 0.02% NaN_3 in PBS. Primary antibodies were incubated overnight at 4 °C with gentle agitation, whereas secondary antibodies were incubated for 1 hour at room temperature. After staining, the supports were washed with PBS. Dishes were imaged directly in PBS, whereas chamber slides were mounted with Fluoromount-G (Invitrogen, Waltham, MA, USA) containing DAPI.

Micrographs were acquired using a Leica TCS-SP8 confocal laser scanning microscope equipped with LAS X software.

4.6 Synchronization

Synchronization was performed using dexamethasone. The culture medium was replaced with DMEM/F-12 containing 100 nM dexamethasone

for 30 minutes. Subsequently, the cells were washed with DMEM/F-12, which was then replaced with the growth medium.

For the assessment of metabolic fluxes using the Seahorse analyzer (see below), separate groups of cell samples plated in a 96-well cartridge were subjected to the synchronization protocol according to a 4-hour staggered schedule, allowing the evaluation of all samples within the same experimental session.

4.7 Analysis of metabolic fluxes and ATP production

Oxygen consumption rate (OCR), extracellular acidification rate (ECAR), and ATP production were measured in derived neurons using a Seahorse XFe96 (Seahorse Bioscience, Billerica, MA, USA). For OCR analysis, the growth medium was replaced with 180 µL of bicarbonate-free DMEM supplemented with 25 mM glucose, 2 mM L-glutamine, 1 mM sodium pyruvate, and 5 mM HEPES, preheated to 37 °C. Cells were pre-incubated for 45 minutes before starting the assay. After measuring basal respiration, oligomycin (1 µM), FCCP (1 µM), and rotenone plus antimycin A (1 µM + 1 µM) were sequentially injected into each well to determine ATP-linked respiration, maximal respiration, and non-mitochondrial oxygen consumption, respectively.

ECAR was measured simultaneously with OCR by including a final injection of 2-deoxyglucose (50 mM) in addition to the compounds listed above. The ATP production rate was determined by first calculating the buffering factor of the assay medium through titration with sequential additions of 5 mM HCl. Subsequently, and as indicated in the manufacturer's protocol, the OCR and ECAR measurements were integrated to derive total ATP production.

OCR, ECAR, and ATP production were normalized for the protein content of each well, measured using the microBCA kit (Thermo Scientific, Waltham, MA, USA).

4.8 Protein measurement

Total protein concentration was determined by the microBCA protein assay (#23235, Thermo Scientific, Waltham, MA, USA), using bovine serum albumin as the standard.

4.9 Real-Time PCR and ddPCR

Total RNA was extracted by using the TRIzol Reagent (#15596026, Invitrogen, Carlsbad, CA, USA) following manufacturer instructions. RNA samples were treated with DNaseI (#18047019, Invitrogen, Carlsbad, CA) and quantified using Nanodrop ND-1000 (Thermo Scientific, Waltham, MA, USA). 1 ug of RNA was reverse transcribed using the iScript cDNA Synthesis kit (Bio-Rad Laboratories, Hercules, California, USA).

qPCR was performed using the SsoAdvanced Universal SYBR Green Supermix (#1725271, Bio-Rad) in a CFX96 Touch Real-Time PCR Detection System (Bio-Rad Laboratories, Hercules, California, USA), with each 10 uL reaction containing 50 ng of cDNA as a template. A technical duplicate was performed for each sample. The relative expression of the target genes was quantified using the comparative threshold cycle ($2-\Delta\Delta Ct$) method and normalized to RNA 18S levels.

ddPCR was performed using EvaGreen Supermix (#1864034, Bio-Rad) on a QX200 Droplet Reader (Bio-Rad Laboratories). Each 20 μL reaction contained 50 ng of cDNA as the template and 150 nM primers. A technical duplicate was performed for each sample. The relative expression of the target genes was normalized to RNA 18S levels.

The following primers from Bio-Rad Laboratories, Qiagen or custom primers were used:

Primer	Company	Reference/Sequence
ARNTL1	Bio-Rad	qHsaCID0023313
NR1D1	Bio-Rad	qHsaCIP0030036
PER2	Bio-Rad	qHsaCID0010055
CLOCK	Bio-Rad	qHsaCID0007280
BMAL2	Qiagen	QT00068250
NPAS2	Bio-Rad	qHsaCID0011719
MFN1	Bio-Rad	qHsaCED0046771
MFN2	Bio-Rad	qHsaCED0004593
DNML1 (DRP1)	Bio-Rad	qHsaCED0057352
OPA1	Bio-Rad	qHsaCED0048382
PINK1	Qiagen	QT00056630
SLC6A3 (DAT1)	Bio-Rad	qHsaCID0006207
TH	Custom	F: GCTGGACAAGTGTCATCACCTG R: CCTGTACTGGAAGGCGATCTCA
RNA 18S	Custom	F: CCTGCGGCTTAATTTGACT R: AGCTATCAATCTGTCAATCCTGTCC

4.10 Morphological analysis of mitochondria

For mitochondrial morphology analysis, cells were cultured on 35 mm glass-bottom dishes and stained with 100 nM TMRE diluted in DMEM/F-12 (#T669, Invitrogen, Carlsbad, CA, USA). After 20 minutes of incubation at 37 °C and 5% CO_2, cells were imaged directly.

Cells were synchronized and imaged using a Leica TCS-SP8 confocal laser scanning microscope. Micrographs were acquired with a 40× immersion objective at 4-hour intervals.

Changes in the mitochondrial network were evaluated using ImageJ software (https://imagej.nih.gov/ij/). The images of the treated cells were converted into binary (black and white) images and, using auto-thresholding, the area (a) and perimeter (p) of the mitochondrial particles were analyzed. Subsequently, the elongation factor (E) and connectivity index (CI) were calculated using the following formulas:

$$E = \frac{p^2}{4\pi \cdot a} \qquad CI = \frac{\sum p}{\sum a}$$

4.11 COSINOR analysis

The following modified COSINOR[95] equation was used to fit the experimental data in synchronized cells:

$$f(t) = M + A \cdot e^{(t \cdot a)} \cdot \cos\left(2\pi \cdot \frac{t - \varphi}{P}\right) + s \cdot t$$

where M = mesor, A = amplitude, a = attenuation factor of A, φ = acrophase, P = period, and s = slope. The best fit was attained using the software GraFit (v 7, Erithacus Software Limited, East Grinstead, West Sussex, UK) by manual insertion of ranges of initial parameters.

4.12 Statistical Analysis

Data are shown as mean ± SEM or mean ± SD. Data were compared by an unpaired Student's t-test with Welch's correction or one-way ANOVA. Differences were considered statistically significant when the p-value was less than 0.05. All analyses were performed using Graph Pad Prism (Graph Pad software, v 10.2.3, San Diego, CA, USA).

5 RESULTS

5.1 iPSC-derived dopaminergic neurons differentiation

Given the nature of Parkinson's disease, dopaminergic neurons represent the most appropriate cellular model, as their physiological characteristics make them the cell type most severely affected by the pathology. They are among the cells with the highest energy demand in the human body and are therefore particularly vulnerable to disruptions in metabolic or mitochondrial homeostasis.

In this context, we first generated induced pluripotent stem cells (iPSCs) from skin fibroblasts obtained from a healthy control and a PD patient[94] and subsequently produced induced neural progenitor cells (iNPCs) from embryoid bodies derived from these iPSCs. The iPSC clones were dissociated and treated for 17 days with an induction medium, followed by a growth medium specific for neural progenitor cells. Microscopic observations revealed the progression of differentiation, during which the iPSCs transitioned from a spherical and compact morphology to a more elongated one (**Figure 8**).

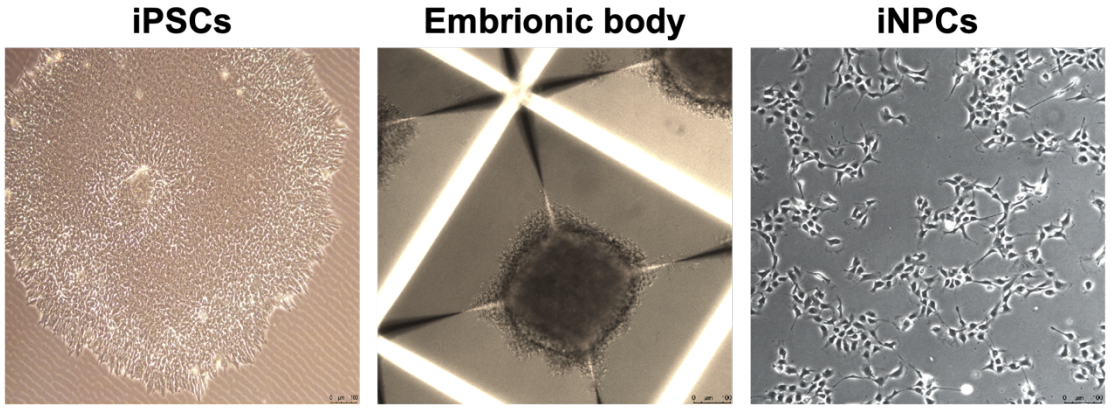

Figure 8: Micrographs

A) Cluster of induced pluripotent stem cells (iPSCs). **B)** Formation of embryonic bodies in AggreWell™800. **C)** Induced neural progenitor cells (iNPCs).

Apparently, the Parkin mutation did not interfere with the reprogramming of fibroblasts into iPSCs, likely because reprogramming into a quiescent stem cell state is characterized by the suppression of mitochondrial oxidative metabolism. In contrast, iNPCs derived from PD patients showed a significantly reduced proliferation rate, suggesting an impairment in the energy-generation system required to sustain cell growth. Subsequently, the differentiation of iPSCs into iNPCs was confirmed by assessing the expression of key markers of these cells, including Nestin, PAX6, and SOX1. Nestin is a cytoskeletal protein expressed in neural precursor cells, whereas PAX6 and SOX1 are transcription factors involved in neural tissue development. The absence of OCT4, a transcription factor characteristic of pluripotent cells, further confirmed the transition from one stem cell state to another (**Figure 9 A**). The iNPCs generated in this manner were further differentiated into dopaminergic neurons. The protocol consisted of 7 days of differentiation followed by 25–30 days of maturation, after which the cells were analysed. Immunocytochemical analysis confirmed the presence of dopaminergic neurons among the differentiated cells. The expression of tyrosine hydroxylase (TH), the key enzyme involved in dopamine synthesis and the primary marker of dopaminergic neurons, as well as MAP2, a somatodendritic protein expressed in mature neurons, was detected (**Figure 9 B**). Using digital droplet PCR (ddPCR), the expression of TH and the dopamine transporter (DAT1) was assessed at different stages of differentiation, confirming that both markers are more highly expressed in differentiated neurons.

By analyzing the ratio between TH and MAP2 transcripts, it was observed that this ratio is lower in neurons carrying the Parkin mutation, suggesting that the mutation reduces the number of dopaminergic neurons generated during differentiation (**Figure 9 C**). Given the high energy demands of these neurons, it can be hypothesized that the mitochondrial dysfunction caused by the absence of Parkin leads to their earlier degeneration.

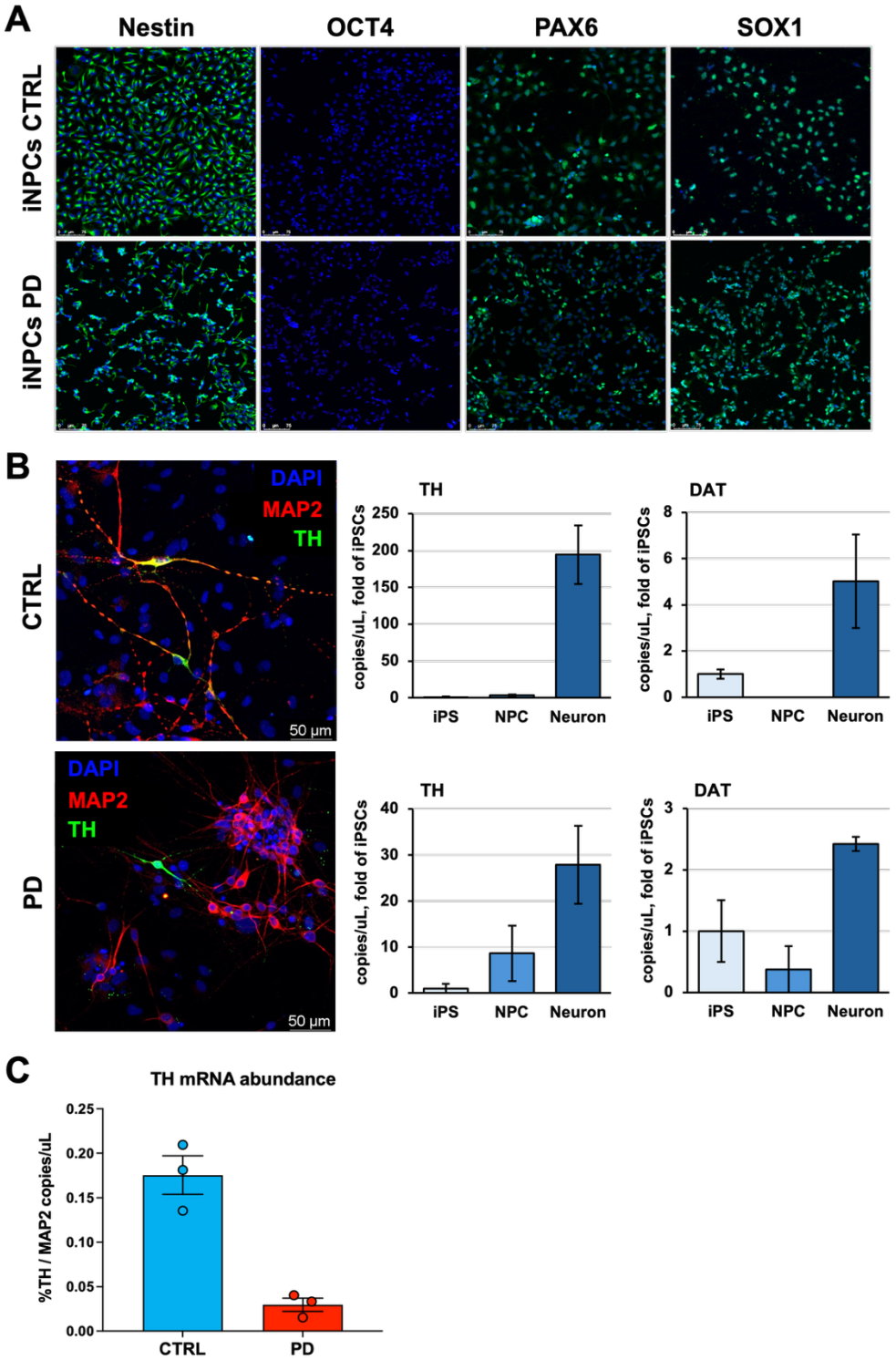

Figure 9: iNPCs and derived-dopaminergic neurons characterization

A) Immunohistochemical analysis of the main markers of iNPCs (Nestin, PAX6, and SOX1) and absence of iPSC markers (OCT4). **B)** Characterization of dopaminergic neurons. Assessment of TH- and MAP2-positive neurons by immunocytochemistry and evaluation of TH and DAT expression at different stages of differentiation using ddPCR. **C)** Ratio of TH to MAP2 transcript levels (ddPCR) in derived neurons. The data show the mean ± SEM of three independent experiments performed in duplicate.

5.2 Expression of clock genes in stem cells

According to several studies, clock genes are poorly expressed in stem cells and their expression increases in differentiated cells.[96] We confirmed these observations by monitoring the expression of BMAL1, one of the core circadian clock genes, from the fibroblasts we reprogrammed through to the fully differentiated neurons. As shown in **Figure 10 A** BMAL1 was more expressed in differentiated cells such as fibroblasts and neurons, while its expression was lower in iPSCs and iNPCs.

Subsequently, the oscillatory profile of BMAL1 was assessed. To this end, the different cell types were subjected to a dexamethasone synchronization protocol to reset the molecular clock, thereby enabling homogeneous synchronization of clock gene expression across the cultured cells once the repression condition was released. In CTRL cells, BMAL1 expression oscillations were more pronounced in derived neurons, as confirmed by COSINOR fitting, which showed a significantly higher oscillation amplitude compared to stem cells. Conversely, in PD cells harboring the Parkin mutation, BMAL1 failed to develop a more pronounced oscillatory pattern in neurons compared to stem cells (**Figure 10 B**).

We then examined the expression of additional clock genes in iPSCs and iNPCs. Comparative analysis of ARNTL1 (BMAL1), NR1D1, PER2, and CLOCK in iPSCs revealed no significant differences between healthy cells and those carrying the Parkin mutation. In iNPCs, however, a non-significant upregulation of all analyzed genes was observed in mutant cells (**Figure 10 C**).

Taken together, these data suggest that the Parkin mutation affects clock gene expression during the transition from a more stem cell-like to a more

differentiated phenotype, as well as the oscillatory pattern of one of the master clock regulators.

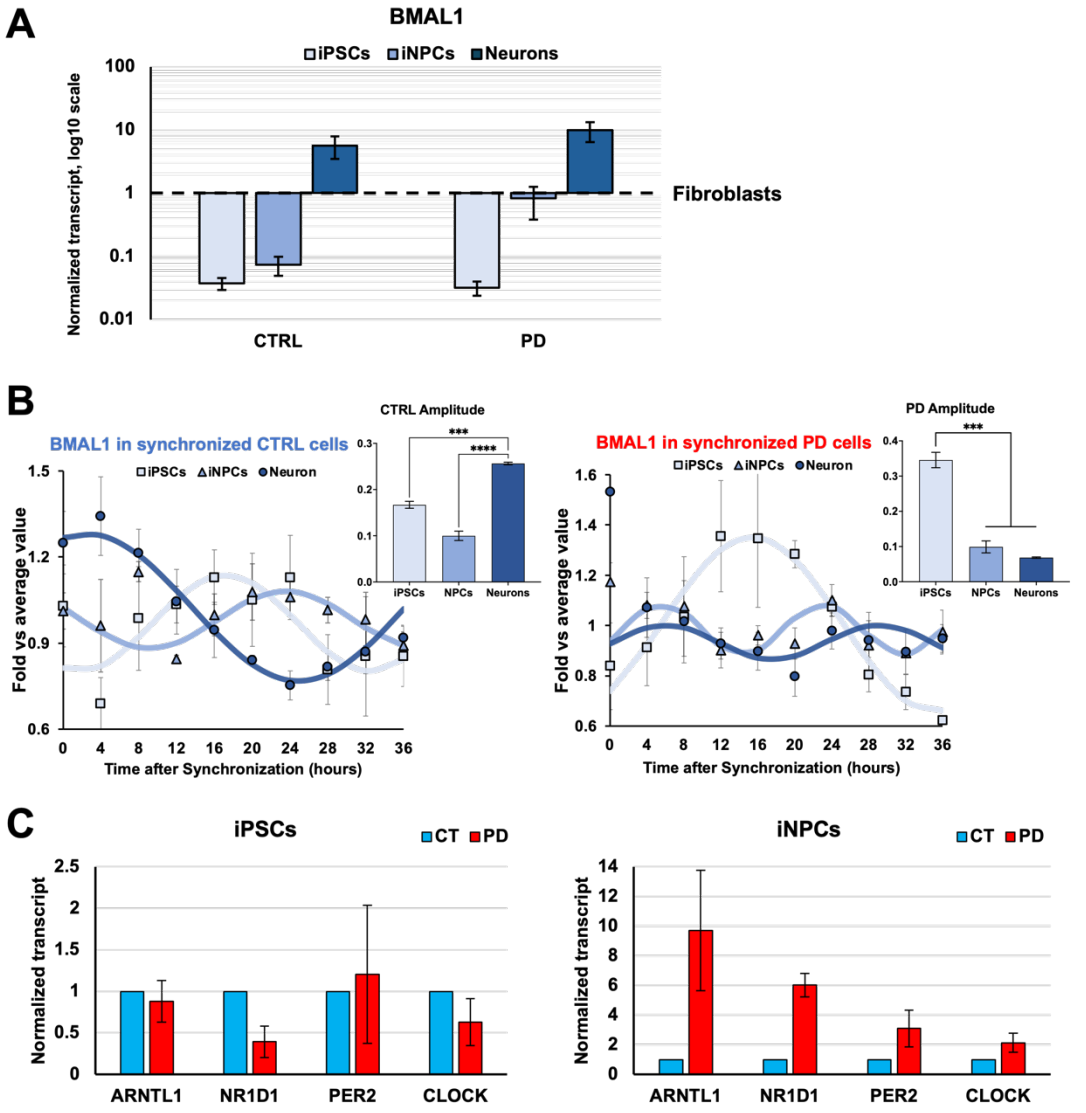

Figure 10: Gene expression analysis of clock genes

A) qPCR analysis of BMAL1 in healthy and affected cells. Data were normalized to housekeeping RNA 18S and expressed as fold-change of the corresponding fibroblasts. Values are shown on a logarithmic scale. **B)** Temporal expression of BMAL1 in synchronized cells. Time points are expressed as fold changes relative to the mean normalized value at time 0. The curves represent the best fit of the COSINOR function, and the bar graphs indicate the amplitude values obtained. **C)** qPCR analysis of clock gene expression in stem cells. The data show the mean ± SEM of three independent experiments performed in duplicate in each condition. Significance was calculated with the one-way ANOVA test (Bonferroni post-hoc); ***p<0.001, **** p<0.0001.

5.3 Circadian clock gene expression is downregulated in Parkin-null derived neurons

Following the above results in stem cells, we investigated the expression levels of the core circadian clock genes in neurons derived from CTRL and PD patients. First, we assessed transcript levels under non-synchronized culture conditions. As shown in **Figure 11 A**, compared with CTRL samples, PD neurons showed no statistically significant differences in the expression of BMAL1, CLOCK, PER2, BMAL2, NPAS2, and NR1D1.

We then measured the expression of core clock genes in cells synchronized with dexamethasone and analyzed their time-dependent profiles using COSINOR fitting. As shown in **Figure 11 B**, synchronized CTRL neurons displayed robust oscillatory expression of all core clock genes with a period close to 24 hours, as well as the expected phase relationships for the repressive branch of the circadian transcriptional feedback loop, as evidenced by the alternating acrophase values.[97]

In contrast, synchronized PD neurons exhibited deregulated expression of all analyzed clock genes, characterized by a statistically significant reduction in oscillation amplitude. Moreover, all genes showed the same acrophase value, indicating a loss of proper phase coordination and impairment of the circadian feedback mechanism.

In addition to the COSINOR fitting, a statistically significant difference between the lowest and highest expression points of the analyzed genes was detected in CTRL cells, whereas no such difference was observed in cells carrying the Parkin mutation (**Figure 11 B**).

These data confirm that the Parkin mutation alters the oscillatory patterns of clock genes but, unlike what was observed in iNPCs, it does not lead to changes in the overall expression levels of these genes.

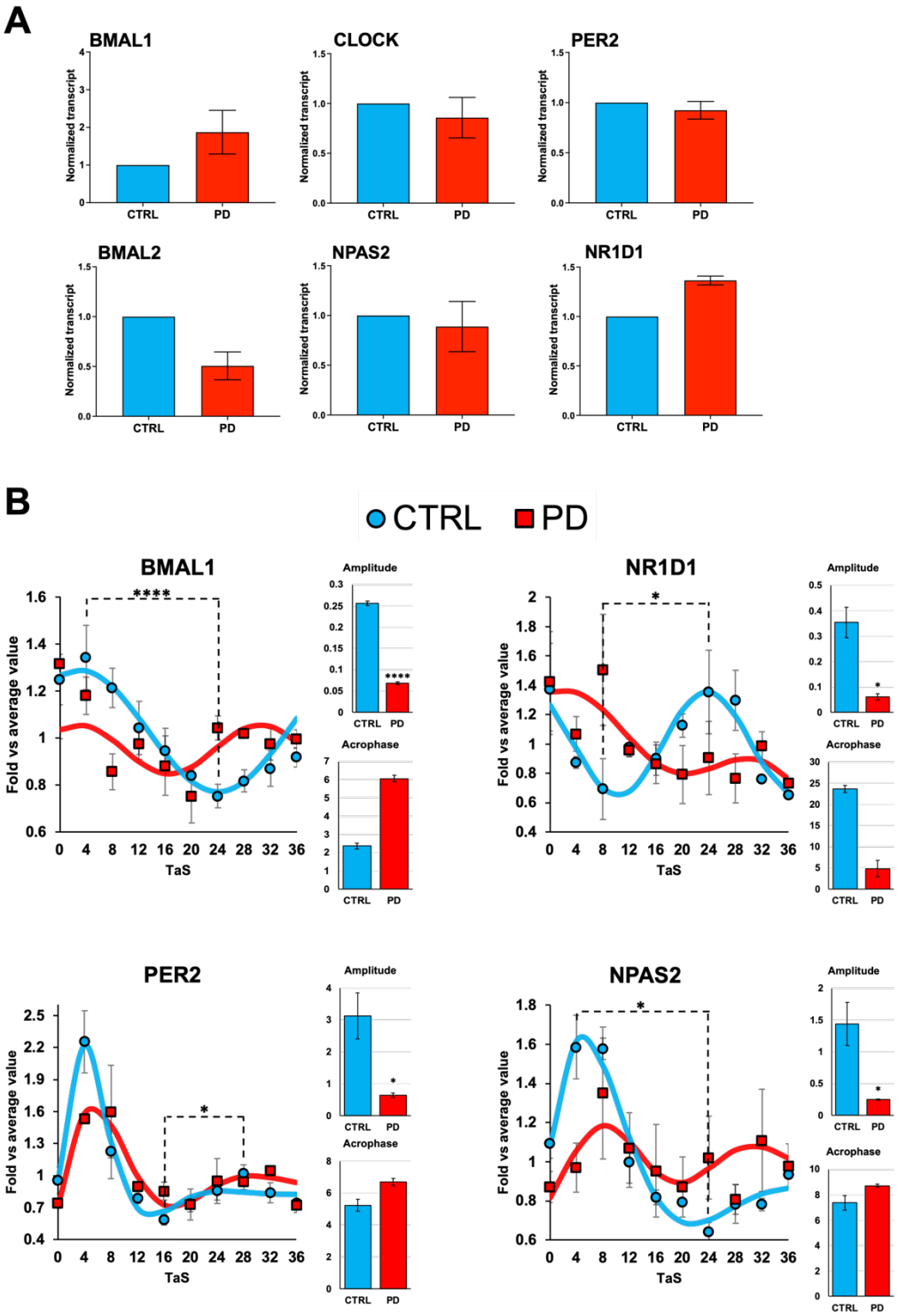

Figure 11: Transcription levels of core clock genes in synchronized derived neurons

A) Transcription levels of core clock genes in derived neurons. Data were normalized to housekeeping gene RNA 18S and expressed as fold-change compared to CTRL. **B)** Temporal expression of core-clock genes in synchronized cells. Time points are expressed as fold changes relative to the mean normalized value at time 0. The curves represent the best fit of the COSINOR function. The data show the mean ± SEM of three independent experiments performed in duplicate in each condition. Significance was calculated with Student's t-test or one-way ANOVA test (Bonferroni post-hoc); *p<0.05, **** p<0.0001.

5.4 Circadian Clock-Dependent Energy Metabolism

Subsequently, the metabolic fluxes of the derived neurons were analyzed**. Figure 12 A, B** show representative OCR (oxygen consumption rate) and ECAR (extracellular acidification rate) recordings under different conditions in control and patient neurons, as assessed using the Seahorse Analyzer. Under basal conditions, a statistically significant reduction in OCR was observed in PD neurons (**Figure 12 C**). The addition of the H^+-ATP synthase inhibitor oligomycin reduced OCR, reflecting the proton leak–dependent respiration. Further addition of the protonophore FCCP increased OCR, which was no longer limited by the mitochondrial membrane potential; however, maximal OCR was significantly higher than basal OCR only in control neurons (**Figure 12 C**). ECAR, an indicator of glycolytic flux, was significantly lower in PD neurons under conditions that maximize glycolysis (i.e., in the presence of oligomycin) (**Figure 12 D**). The glycolytic reserve was also significantly reduced in PD neurons, thereby demonstrating a lack of metabolic switch to compensate the respiratory deficit. Taken together, these findings reveal a general impairment of bioenergetic functions in neurons from PD patient, which becomes particularly evident when the cells are examined under stress conditions.

To verify whether the molecular alteration of circadian genes also resulted in a functional impairment, we analyzed metabolic fluxes in synchronized neurons.

As shown in **Figure 12 E, F**, healthy-derived neurons displayed clear rhythmic and in-phase oscillations of both basal OCR and ECAR. In contrast, PD neurons exhibited a markedly dampened rhythmicity of metabolic fluxes. Specifically, PD neurons showed a significant reduction in the mesor and amplitude parameters of OCR, as well as an increased period compared to CTRL. Regarding the glycolytic flux, only the mesor parameter was significantly lower in PD neurons.

Consequently, the bioenergetic profiles of PD and control neurons showed distinct metabolic patterns (**Figure 13**): CTRL neurons exhibited oscillations in the energetic state, whereas the metabolic fluxes of PD neurons remained confined to the low-energy region of the bioenergetic profile.

In summary, extending the analysis of metabolic fluxes to synchronized cells allowed us to uncover an additional aspect of the dysfunctions caused by parkin alteration. Healthy neurons displayed similar oscillatory patterns of OCR and ECAR; in contrast, neurons with parkin mutations showed a drastic reduction in the rhythmic pattern of metabolic fluxes, confirming that mutation of this protein disrupts the interaction between the molecular clock and mitochondrial metabolism.

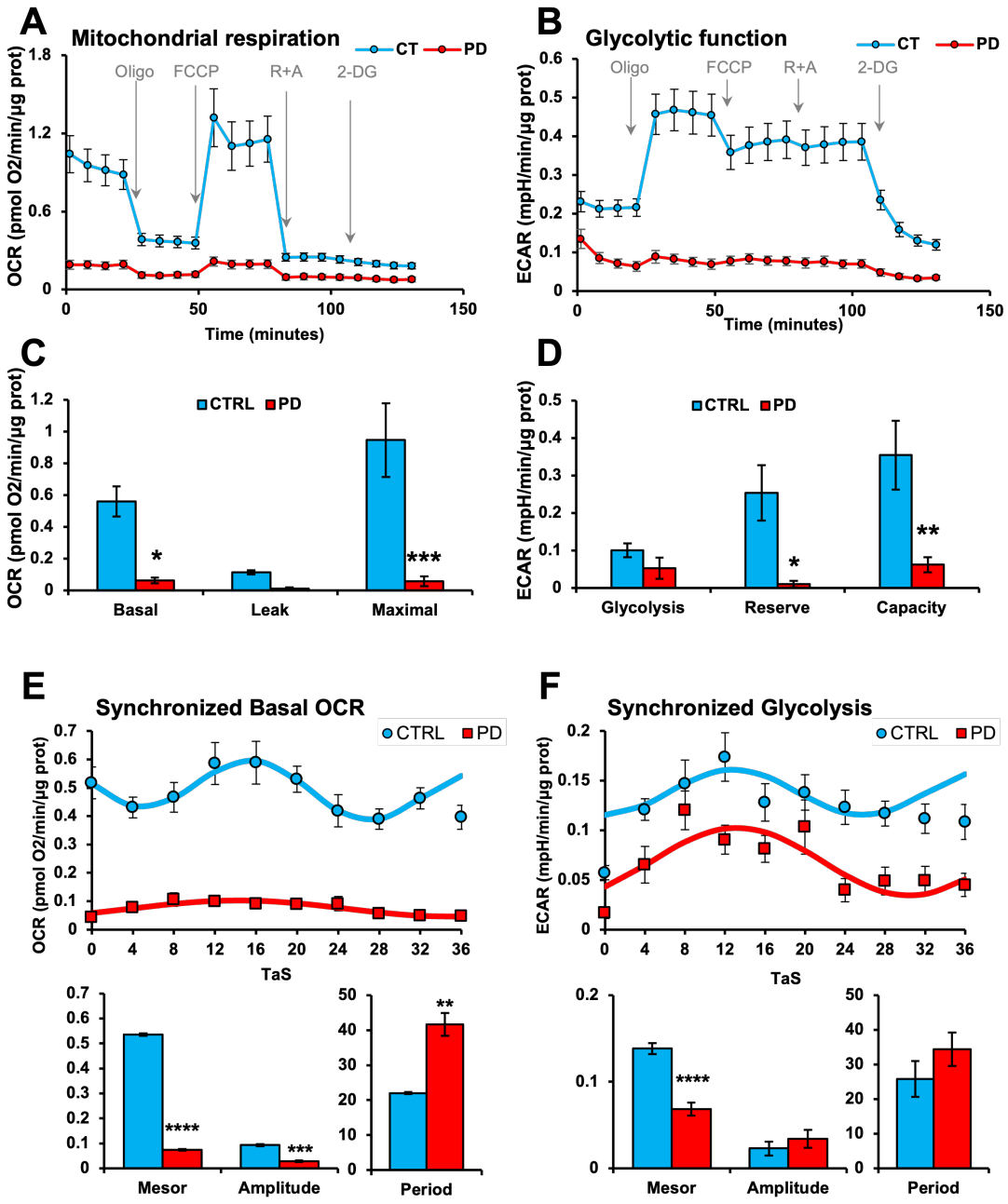

Figure 12: Energy metabolism in derived dopaminergic neurons

A, B) rack generated by the Seahorse XF Analyzer showing OCR (A) and ECAR (B). For each trace, after the baseline measurement, oligomycin A (oligo), FCCP, rotenone + antimycin A (R+A), and 2-deoxyglucose (2-DG) were added as indicated by the arrows. **C, D)** The bar graphs show the data obtained from the experiments shown in (A, B). **C)** Basal: OCR at rest; leak: OCR measured in the presence of oligomycin; maximal: OCR measured in the presence of FCCP. OCR values were corrected for residual OCR measured in the presence of rotenone and antimycin A. **D)** Glycolysis: ECAR at rest; capacity: ECAR measured in the presence of oligomycin; reserve: difference between maximal and basal glycolysis. ECAR values were corrected for residual ECAR measured in the presence of 2-deoxyglucose. **E)** Basal OCR and

F) Basal ECAR in synchronized neurons. Time points were fitted with the COSINOR function. Histograms show the mesor, amplitude, and period for respiration (E) and glycolysis (F) of the best-fitting COSINOR. The data show the mean ± SEM of three independent experiments performed in quadruplicate. Statistical significance was calculated using one-way or two-way ANOVA; * p <0.05, ** p <0.01, *** p <0.001, **** p<0.0001 vs. CTRL cells.

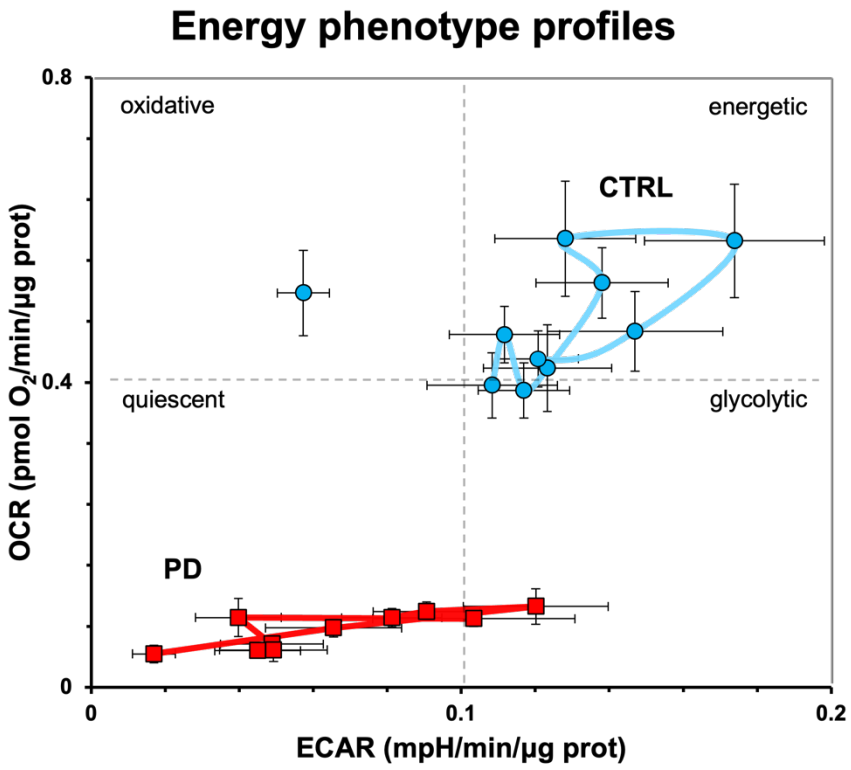

Figure 13: Bioenergetic profiles in synchronized neurons

The graph shows the energy map obtained by plotting the baseline values of oxygen consumption rate (OCR) and extracellular acidification rate (ECAR) obtained from the data shown in **Figure 25** for healthy neurons (blue circle) and PD patient (red square).

5.5 ATP production is downregulated in PD neurons

ATP is the primary energy currency of the cell and is essential for sustaining virtually all cellular processes. It provides the energy required for biosynthetic reactions, ion transport across membranes, cytoskeletal dynamics, and signal transduction. Neurons, in particular, rely heavily on ATP to maintain membrane potential and support synaptic transmission. Because

mitochondria are the main source of ATP through oxidative phosphorylation, any alteration in their function has immediate consequences on cellular homeostasis and viability. We wanted to determine whether the reduction in respiratory activity observed in PD neurons translated into an actual decrease in ATP production. To address this, we used a modified Seahorse protocol (see Materials and Methods), which allowed us to quantify the rate of ATP production in our derived neurons. Quantification of unsynchronized neurons showed that ATP produced through OXPHOS (Mito ATP) was significantly reduced in PD neurons compared to controls, while no difference was observed in ATP produced via glycolysis (Glyco ATP) (**Figure 14 A**). Overall, total ATP levels were markedly lower in PD neurons than in controls, confirming that dysfunction in the mitochondrial quality control system results in impaired energy production. We then assessed ATP production in synchronized cells and, consistent with the metabolic flux analysis, only the Mito ATP of control neurons displayed a more robust oscillatory pattern (**Figure 14 B**). In contrast, both Mito ATP and Glyco ATP oscillations were almost completely absent in neurons carrying Parkin mutation.

The parameters obtained from the COSINOR fitting show a significant reduction in both Mito ATP and Glyco ATP mesor in PD neurons, as well as a statistically significant decrease in Mito ATP amplitude in neurons carrying the mutation (**Figure 14 C**).

The data obtained from the ATP production assessment further confirm the energy production defect in PD neurons. This marked reduction in ATP levels may result in an insufficient energy supply to sustain dopaminergic neuron development, potentially explaining the previously observed decrease in TH transcript levels in PD cells.

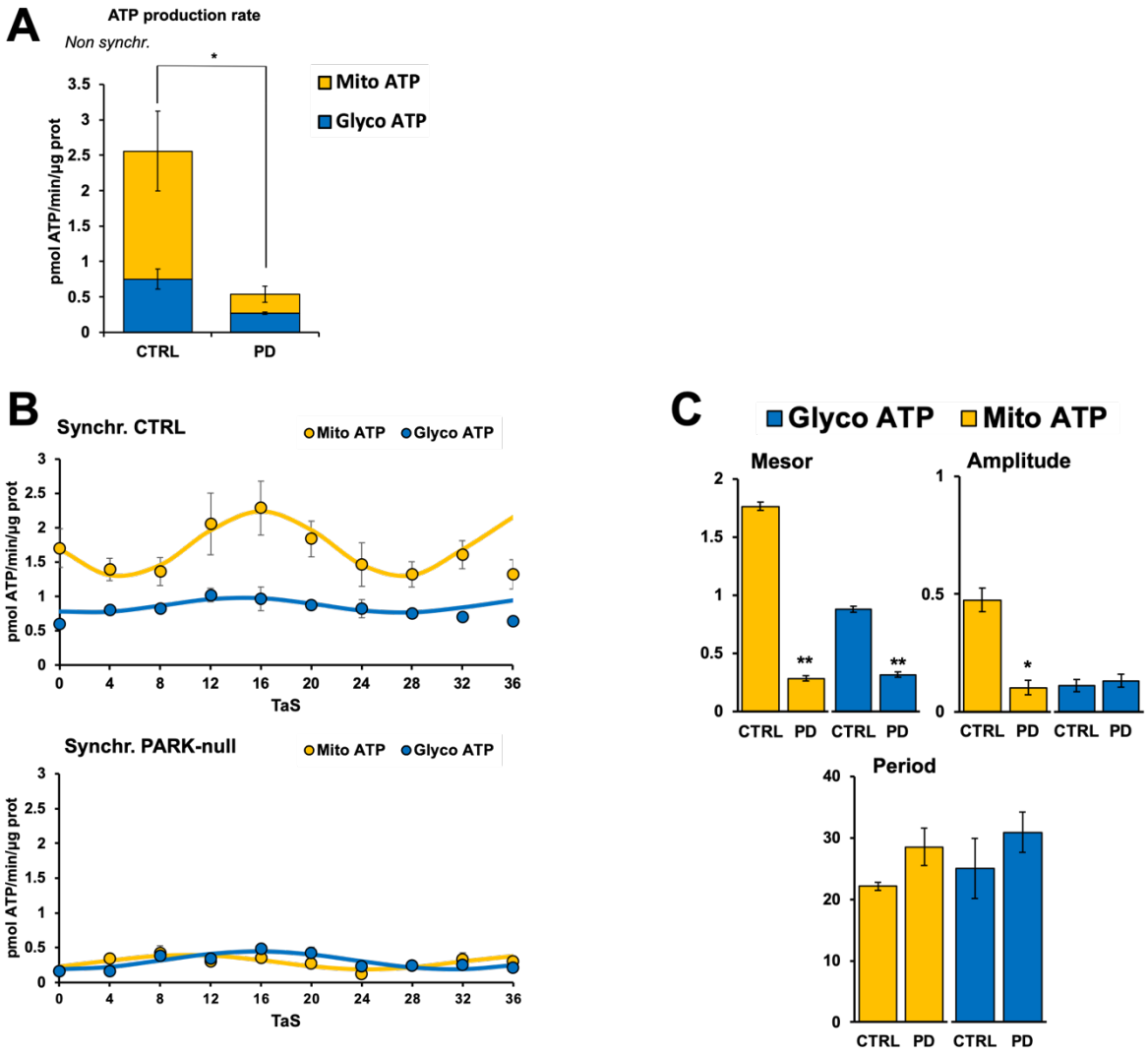

Figure 14: ATP production in derived neurons

A) ATP production rate through mitochondrial respiration (Mito ATP) and glycolysis (Glyco ATP) in derived neurons. **B)** ATP production rate in synchronized neurons. **C)** Histograms show the mesor, amplitude, and period for Mito ATP and Glyco ATP of the best-fitting COSINOR. The data show the mean ± SEM of two independent experiments performed in quadruplicate. Statistical significance was calculated using two-way ANOVA; * $p < 0.05$, ** $p < 0.01$ vs. CTRL cells.

5.6 Alterations in mitochondrial dynamics

Several studies have shown that the molecular clock exerts a regulatory function on mitochondrial homeostasis and that, in turn, mitochondrial activity can influence the expression of clock genes. The ability of mitochondria

to produce energy is closely linked to their abundance and morphology, which depend on biogenetic, mitophagic, and dynamic processes. A common denominator of these processes is the PINK1/Parkin pathway, a sequential mechanism that coordinates multiple aspects of mitochondrial quality control.[52] Given the importance of this pathway, we investigated whether alterations in mitochondrial quality control could affect the circadian rhythm of mitochondrial morphology.

The ability of mitochondria to produce energy is also linked to their morphology, which is regulated by dynamic fusion and fission processes. Notably, the mitochondrial network undergoes cyclical changes, shifting from a more fused and elongated state to a more fragmented one. These oscillations have been shown to be largely controlled by the clock gene PER2.[88] Considering the results obtained from the analyses of mitochondrial metabolism and clock gene expression, we next examined changes in the morphology of the mitochondrial network in neurons from control subjects and PD patients.

To evaluate mitochondrial network morphology, neurons were synchronized and subsequently stained with the mitochondrial probe TMRE. The cells were then imaged by confocal microscopy, acquiring one image every 4 hours for a total duration of 36 hours. Finally, the perimeter (p) and area (a) of the mitochondria were evaluated, and the elongation ($\mathbf{E = p^2/4\pi a}$) and connectivity index ($\mathbf{CI = \sum p/\sum a}$) were calculated.

Figure 15 A shows a representative selection of images at different time points post-synchronization, illustrating the mitochondrial network of control and PD neurons in both elongated and fragmented states.

Figure 15 B shows the time profiles of Elongation and CI, along with the best COSINOR fit. Control cells displayed larger oscillations compared to PD cells. Consistent with the previous results, patient-derived neurons did not exhibit a significant change in oscillation period but showed a statistically significant reduction in both amplitude and mesor compared with controls.

These results further confirm that altered mitochondrial quality control leads to impairments in both bioenergetic function and mitochondrial dynamics. PD mitochondria appear more fragmented than those of controls and fail to exhibit time-dependent oscillatory behavior.

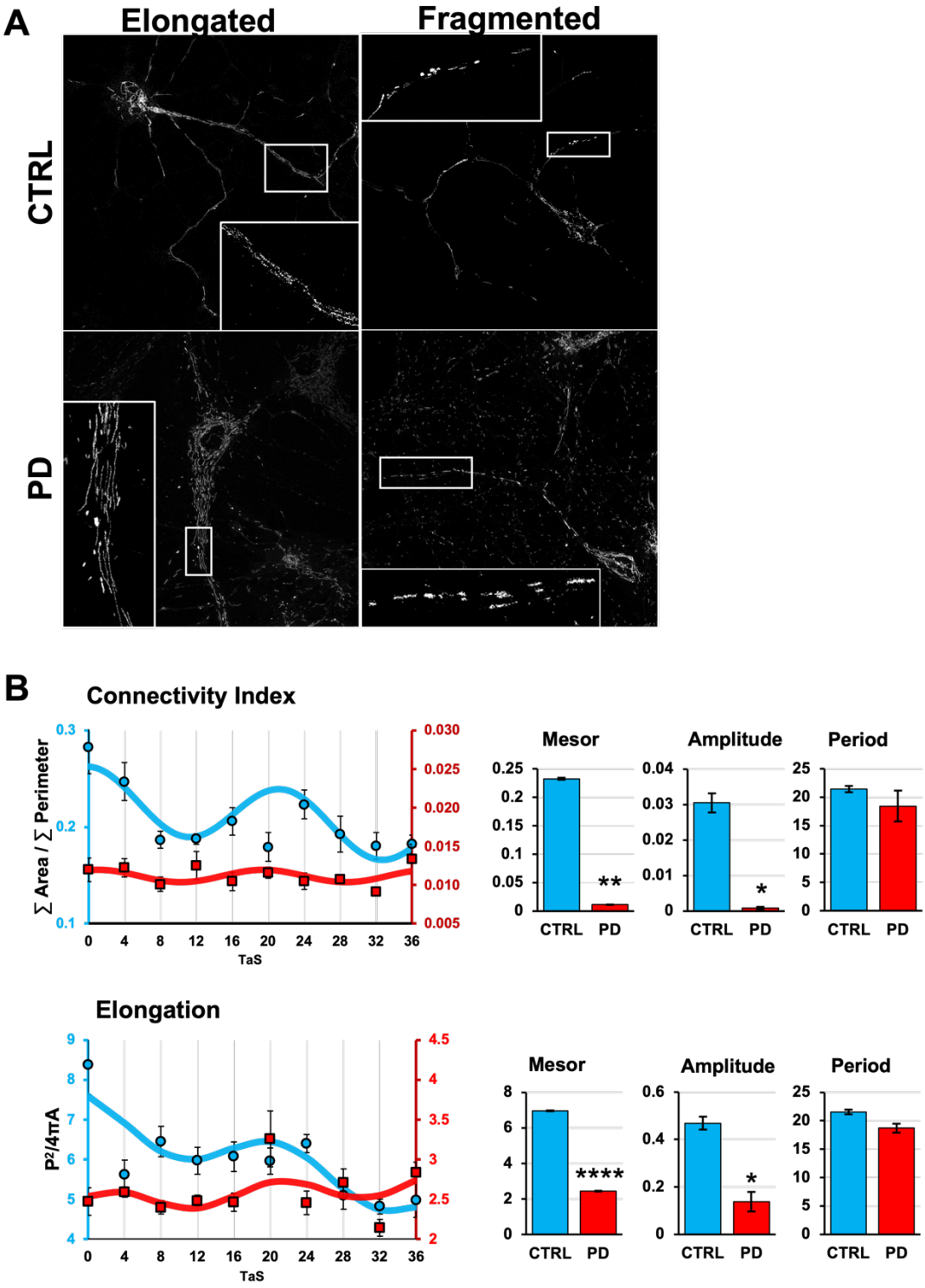

Figure 15: Mitochondrial morphology

A) Mitochondrial morphology in synchronized neurons. The images show the transition from a more fragmented network to a more interconnected one at different time points after

synchronization. **B)** Elongation and Connectivity index (CI) of the mitochondrial network in normal (CTRL) neurons and neurons derived from PD patients synchronized with dexamethasone. Time points were fitted using the COSINOR function. The histograms show the mesor, amplitude, and period for elongation and CI of the best-fitting COSINOR. Data represent the mean ± SEM of two independent experiments performed in triplicate. Statistical significance was determined using Student's t-test; * $p < 0.05$, ** $p < 0.01$, **** $p < 0.0001$ vs. control cells.

5.7 Assessment of genes involved in mitochondrial dynamics

To further confirm the previous results, we assessed whether the oscillatory variations observed in mitochondrial morphology were accompanied by changes in the expression of the genes most involved in fusion and fission processes. To this end, we evaluated the expression levels of DRP1, Mitofusins (MFN1 and MFN2), OPA1, and PINK1.

DRP1 is a GTPase normally involved in mitochondrial fission, and its activity can be either activated or inhibited through post-translational phosphorylation/dephosphorylation. MFN1 and MFN2 are proteins located on the outer mitochondrial membrane that mediate outer membrane fusion through the formation of homo- or heterodimers. OPA1 is a GTPase responsible for inner mitochondrial membrane fusion and cristae formation. Finally, PINK1 is a serine/threonine kinase that, together with Parkin, regulates the process of mitophagy.

Figure 16 shows the results obtained from the gene expression analysis in unsynchronized cells (**Figure 16 A**) and in synchronized cells with the corresponding COSINOR fitting (**Figure 16 C**). At the basal level, only the DRP1 and PINK1 genes displayed statistically significant overexpression in PD neurons compared with CTRL.

When analyzing the circadian expression profiles, the same genes, DRP1 and PINK1, exhibited deregulated oscillations in PD neurons, characterized by a statistically longer oscillation period. It should be noted that no difference was found in the oscillations of the genes involved in the fusion processes.

These results may indicate a general increase in the mitochondrial fission process, likely aimed at removing damaged mitochondria in neurons carrying the Parkin mutation. However, given that the mitophagy pathway is impaired precisely because of the absence of Parkin, the increase in fission ultimately results in the accumulation of mitochondria that cannot be cleared by the cell, a reduction in OXPHOS efficiency, and, ultimately, the death of these neurons.

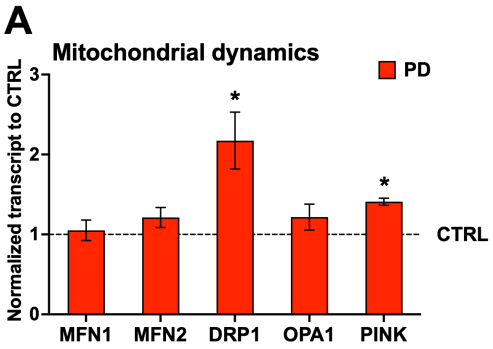

B

ΔCT	Mean of CTRL	Mean of PD	P value	Below threshold ?
MFN1	7,782	7,731	0,922509	No
MFN2	10,35	10,09	0,673514	No
DRP1	**6,413**	**5,332**	**0,028223**	*
OPA1	8,025	7,767	0,499655	No
PINK1	**10,04**	**9,549**	**0,035819**	*

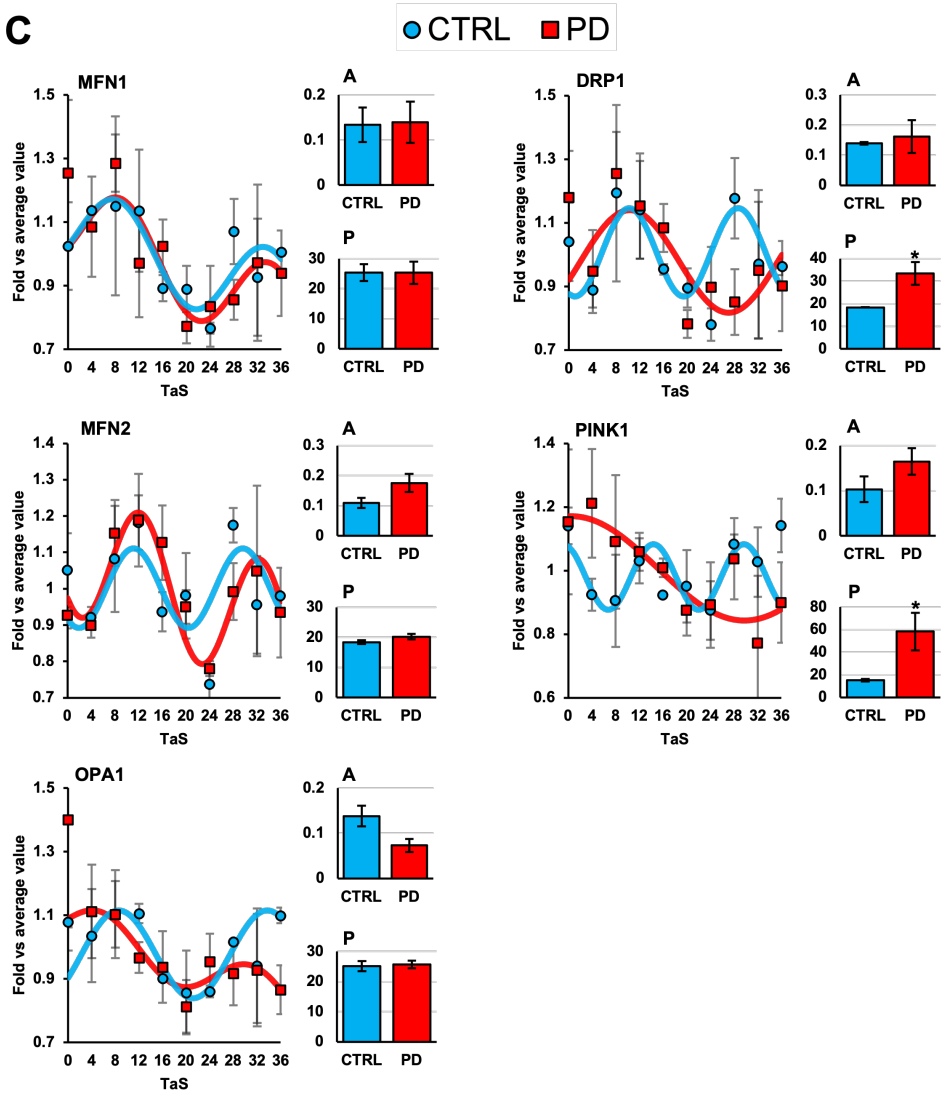

Figure 16: Genes involved in mitochondrial dynamics

A) Transcription levels genes involved in mitchondrial dynamics in derived neurons. Fusion process: MFN 1 and 2 and OPA1; fission process: DRP1; mitophagy: PINK1. Data were

normalized to housekeeping gene RNA 18S and expressed as fold-change compared to CTRL. **B)** Statistical analysis of the ΔCTs of the genes of **A**. C) Temporal expression MFN1/2, OPA1, DRP1 and PINK1 genes in synchronized cells. Time points are expressed as fold changes relative to the mean normalized value at time 0. The histograms show the amplitude (A) and period (P) obtained from the best fitting COSINOR. The curves represent the best fit of the COSINOR function. The data show the mean ± SEM of three independent experiments performed in duplicate. Significance was calculated with Student's t-test; *$p<0.05$.

6 DISCUSSION

Growing evidence from both basic research and clinical studies indicates that circadian rhythmicity is disrupted in Parkinson's disease (PD) at behavioral, physiological, and molecular levels. Circadian dysfunction has been consistently reported in PD patients as well as in experimental models[89], leading to disturbances in systemic homeostasis that may further aggravate disease progression. In particular, several studies have documented alterations in sleep–wake cycles, visual performance, and daily hormone secretion patterns[89], all of which reflect an impaired temporal organization of physiological processes. These findings are not unexpected given the central role of dopamine in circadian regulation and, conversely, the influence of circadian pathways on dopamine synthesis, release, and turnover.[98]

Despite these observations, the molecular mechanisms linking circadian disruption to neurodegeneration remain incompletely understood. Considering that mitochondrial function exhibits intrinsic rhythmicity, and that mitochondrial impairment is a hallmark of PD, we designed this study to investigate the interaction between circadian clock circuits and cellular metabolism in parkin-null iPSC-derived neurons generated from PD patients.

Similar to what has already been demonstrated on fibroblasts isolated from PD patients by Pacelli et al.[93], our results confirm that Parkin (PARK2) deficiency in human iPSC-derived dopaminergic neurons produces a multi-level disruption that couples impaired mitochondrial quality control with bioenergetic failure and collapse of circadian regulation. PD neurons in our study showed reduced basal and maximal mitochondrial respiration, decreased mitochondrial ATP production, impaired ability to increase glycolysis under stress, and a markedly reduced capacity to exhibit time-of-day oscillations in both metabolic fluxes and ATP levels (**Figure 12-14**). These functional impairments were accompanied by increased mitochondrial fragmentation, loss of rhythmic fusion–fission cycles, and dumped clock-gene oscillations

after dexamethasone synchronization (reduced amplitude and loss of normal phase relationships) (**Figure 11**).

Mechanistically, these observations are consistent with a model in which defective Parkin-dependent mitophagy leads to accumulation of damaged mitochondria that cells attempt to resolve by upregulating fission (DRP1), but because the clearance machinery is compromised the net effect is persistent fragmentation and reduced OXPHOS efficiency. The central role of the PINK1–Parkin pathway in recruiting Parkin to depolarized mitochondria and initiating mitophagy is well established (PINK1 phosphorylates both ubiquitin and Parkin to prime recruitment and activation), providing a molecular basis for how PARK2 mutations can impair mitochondrial turnover.[68,99]

The connection between altered dynamics and circadian biology has been described in recent studies showing that DRP1 activity is rhythmically regulated and that circadian modification of DRP1 is necessary for daily oscillations in mitochondrial morphology and ATP production.[88] Loss or mis-timing of DRP1 phosphorylation disrupts the normal diurnal changes in mitochondrial form and function, which we observe phenocopying in Parkin-mutant neurons (**Figure 15**). Thus, the altered DRP1 expression/oscillation we measured provides a plausible mechanistic link between impaired mitochondrial dynamics and the disrupted metabolic rhythms in PD neurons (**Figure 16**).

Clock machinery components themselves (for example BMAL1) are known regulators of mitochondrial function and quality control via metabolic and transcriptional axes (SIRT1/PGC-1α and related pathways), and conversely, mitochondrial metabolic state feeds back onto clock function through NAD^+/SIRT signaling and redox-sensitive factors.[53,86] Our data — dumped clock oscillations in synchronized PD neurons without major steady-state transcript differences in the non- synchronized condition (**Figure 11**) — are consistent with a model in which mitochondrial dysfunction perturbs

metabolic coupling mechanisms that normally entrain and amplify clock gene rhythms (for example via NAD^+/SIRT1 or AMPK pathways).

The use of patient-derived iPSC models has previously shown that PARK2 mutations recapitulate mitochondrial abnormalities and selective dopaminergic vulnerability, supporting the translational relevance of the cellular phenotypes we observe.[100] Our finding of a reduced TH/MAP2 ratio and impaired differentiation/survival of dopaminergic neurons in the Parkin background is therefore in line with earlier iPSC studies and strengthens the idea that impaired mitochondrial quality control contributes directly to the selective loss of dopaminergic neurons in PD (**Figure 9**).

Together, these results suggest several actionable implications. First, restoring mitophagic flux (for example by rescuing Parkin function or by activating Parkin-independent mitophagy pathways) could reduce the burden of damaged mitochondria, rebalance fusion–fission dynamics, and thereby recover OXPHOS capacity and circadian rhythmicity. Second, direct modulation of DRP1 activity or its post-translational regulation may re-establish healthier mitochondrial networks and improve ATP output. Third, combined strategies that both improve mitochondrial clearance and support metabolic resilience (NAD^+ boosters, mitochondrial antioxidants, or substrates/cofactors) may be necessary to restore neuronal energy homeostasis and improve survival. These therapeutic ideas are grounded in both our data and the broader literature on Parkin/PINK1 biology and circadian control of mitochondrial dynamics.[88,99]

Key limitations in our study include the small number of iPSC lines used and the *in vitro* nature of the synchronization assay. Validation across additional patient and isogenic control lines would test generality and exclude line-specific effects. *In vivo* confirmation would further strengthen translational claims. Mechanistically, our transcriptional and functional data implicate altered mitophagy and fission, but direct dynamic readouts of mitophagic flux (e.g., mito-Keima or mito-QC reporters), Parkin

recruitment/ubiquitination assays, and detailed mapping of DRP1 phosphorylation states are needed to prove causality. Some targeted experiments that could directly address causality and identify potential therapeutic targets include:

1. genetic rescue of Parkin in patient neurons and assessment of mitochondrial, metabolic and clock readouts;
2. live-cell mitophagy flux measurements;
3. genetic/pharmacological modulation of DRP1 to determine whether reducing fragmentation restores OXPHOS and rhythms;
4. time-resolved proteomics/metabolomics to identify downstream effectors linking metabolic collapse to clock disruption.

Beyond molecular rescue, our results highlight the potential value of chronobiological perspectives in PD. Disruption of cellular clocks may underlie daily variability in symptoms and medication responsiveness reported clinically; if mitochondrial and clock dysfunction extend to peripheral tissues, circadian biomarkers (timed gene expression, metabolite rhythms, actigraphy) could become useful readouts of disease state or therapeutic response. Chronotherapeutic strategies — timing treatments to the patient's residual rhythmicity or to phases of maximal metabolic reserve — may enhance efficacy and reduce toxicity and deserve preclinical testing in synchronized patient-derived models.

In sum, our study provides convergent functional, transcriptional, and morphological evidence that Parkin deficiency produces a coupled breakdown of mitochondrial quality control, bioenergetic competence, and circadian regulation in human dopaminergic neurons. This tri-partite dysfunction plausibly contributes to impaired differentiation and selective vulnerability of dopaminergic neurons in PARK2-linked PD. Targeting the intersecting nodes of mitophagy (PINK1/Parkin), fusion–fission balance (DRP1/MFNs/OPA1), and metabolic–clock coupling may therefore offer promising avenues to restore cellular energy homeostasis and preserve neuronal function.

7 CONCLUSION

The results obtained in this study show that Parkinson's disease can profoundly affect the autonomous rhythmic processes of cells. In particular, the parkin mutation disrupts metabolic fluxes, mitochondrial dynamics, and molecular clock mechanisms.

At the mitochondrial level, due to its central role in quality control, parkin dysfunction leads to a general impairment of mitochondrial energy functions and a loss of metabolic switching capacity in affected cells. The effects on the molecular clock become especially evident after in vitro synchronization of mutated and control neurons: their comparison revealed a marked reduction in the rhythmic patterns of metabolic fluxes and mitochondrial dynamics, with PD neurons displaying a tendency toward more fragmented mitochondria and remaining confined to a quiescent energetic state.

The accumulation of damaged mitochondria, combined with the inability to remove them through mitophagy, contributes to reduced mitochondrial respiration and ultimately to cell death. Disruption of mitochondrial homeostasis also results in the breakdown of the circadian clock feedback system, leading to the loss of the normal oscillatory patterns of clock gene expression observed in healthy cells (**Figure 17**).

From observations made during differentiation, it appears that the parkin mutation influences the neurogenesis process of iPSCs; nevertheless, our results confirmed the feasibility of generating a cellular model suitable for studying the dysfunctions caused by parkin. Further research is needed to better define the molecular mechanisms underlying the interaction between mitochondrial energy metabolism, circadian clock circuits, and the pathophysiology of Parkinson’s disease. Moreover, our findings suggest a role for parkin in these interactions, adding an additional layer of complexity to the neurodegenerative processes associated with this protein.

Finally, one of our future goals is to identify new targets for chronotherapeutic strategies aimed at restoring mitochondrial homeostasis and circadian clock function in order to slow the degeneration of dopaminergic neurons.

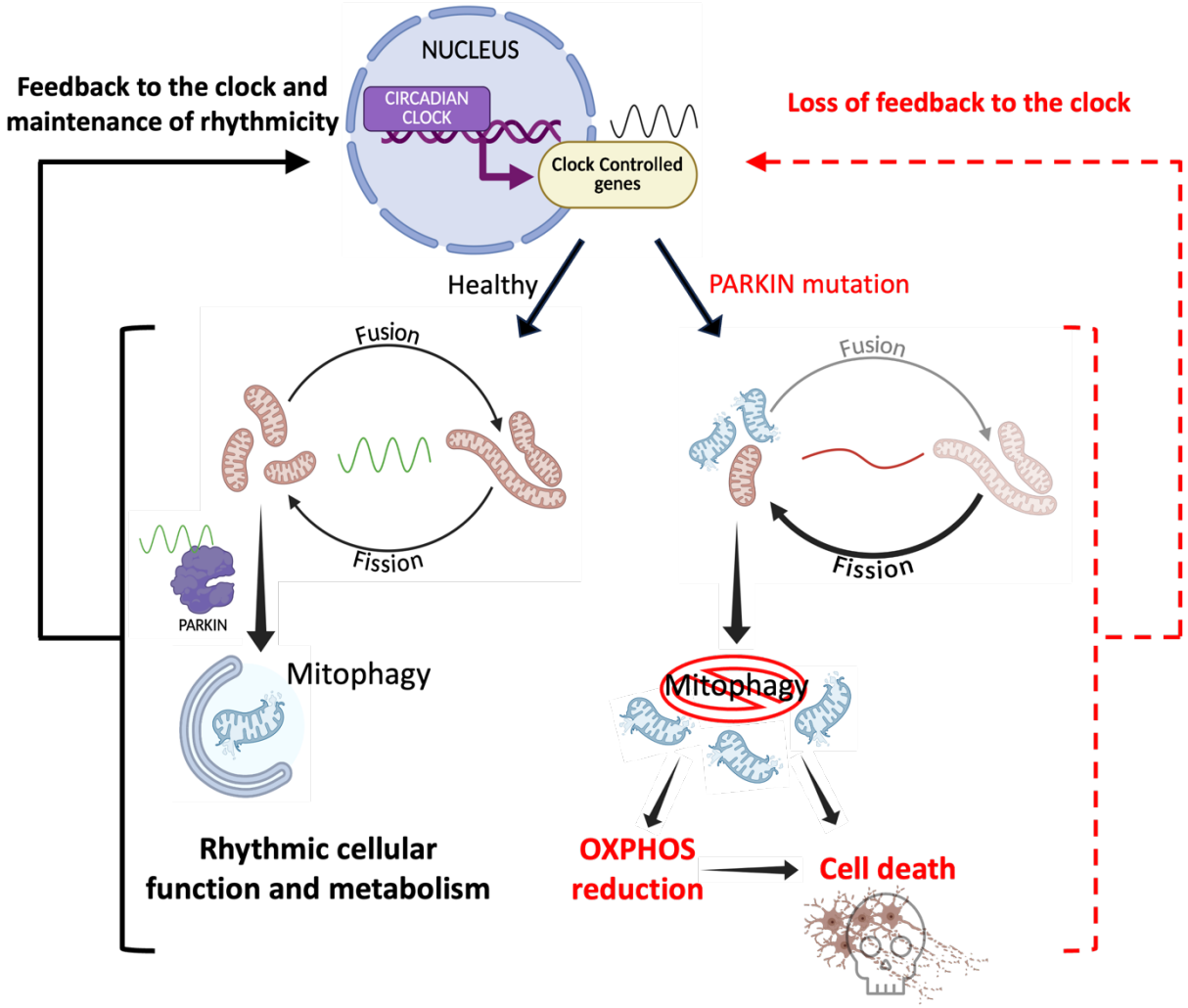

Figure 17: Graphical conclusion

8 REFERENCES

1. Deng, H., Wang, P. & Jankovic, J. The genetics of Parkinson disease. *Ageing Research Reviews* **42**, 72–85 (2018).
2. Poewe, W. *et al.* Parkinson disease. *Nat Rev Dis Primers* **3**, 17013 (2017).
3. Sveinbjornsdottir, S. The clinical symptoms of Parkinson's disease. *Journal of Neurochemistry* **139**, 318–324 (2016).
4. Kalia, L. V. & Lang, A. E. Parkinson's disease. *The Lancet* **386**, 896–912 (2015).
5. De Virgilio, A. *et al.* Parkinson's disease: Autoimmunity and neuroinflammation. *Autoimmunity Reviews* **15**, 1005–1011 (2016).
6. Pankratz, N. & Foroud, T. Genetics of Parkinson disease. *Genetics in Medicine* **9**, 801–811 (2007).
7. Jagadeesan, A. J. *et al.* Current trends in etiology, prognosis and therapeutic aspects of Parkinson's disease: a review. 14 (2017).
8. Rosner, S., Giladi, N. & Orr-Urtreger, A. Advances in the genetics of Parkinson's disease. *Acta Pharmacol Sin* **29**, 21–34 (2008).
9. Lesage, S. & Brice, A. Parkinson's disease: from monogenic forms to genetic susceptibility factors. *Hum Mol Genet* **18**, R48–R59 (2009).
10. Noyce, A. J. *et al.* Meta-analysis of early nonmotor features and risk factors for Parkinson disease. *Annals of Neurology* **72**, 893–901 (2012).
11. Benkler, M., Agmon-Levin, N. & Shoenfeld, Y. Parkinson's disease, autoimmunity, and olfaction. *International Journal of Neuroscience* **119**, 2133–2143 (2009).
12. Møller, A., Perrild, H., Pedersen, H. & Høier-Madsen, M. Parkinson's disease and autoimmunity. *Acta Neurologica Scandinavica* **79**, 173–175 (1989).

13. Liu, B., Gao, H.-M. & Hong, J.-S. Parkinson's disease and exposure to infectious agents and pesticides and the occurrence of brain injuries: role of neuroinflammation. *Environ Health Perspect* **111**, 1065–1073 (2003).

14. Fiszer, U. *et al.* γδ+ T cells are increased in patients with Parkinson's disease. *Journal of the Neurological Sciences* 7 (1994).

15. Kalinderi, K., Bostantjopoulou, S. & Fidani, L. The genetic background of Parkinson's disease: current progress and future prospects. *Acta Neurol Scand* **134**, 314–326 (2016).

16. Liao, Q. *et al.* MTHFR C677T variant reduces risk of sporadic Parkinson's disease in ethnic Chinese. *Acta Neurol Scand* **130**, e30–e34 (2014).

17. Krebs, C. E. & Paisán-Ruiz, C. The Use of Next-Generation Sequencing in Movement Disorders. *Front Genet* **3**, (2012).

18. Wang, Z., Liu, X., Yang, B.-Z. & Gelernter, J. The Role and Challenges of Exome Sequencing in Studies of Human Diseases. *Front. Genet.* **4**, (2013).

19. Blauwendraat, C., Nalls, M. A. & Singleton, A. B. The genetic architecture of Parkinson's disease. *The Lancet Neurology* **19**, 170–178 (2020).

20. Polymeropoulos, M. H. Mutation in the Synuclein Gene Identified in Families with Parkinson's Disease. *Science* **276**, 2045–2047 (1997).

21. Kitada, T. *et al.* Mutations in the parkin gene cause autosomal recessive juvenile parkinsonism. *Nature* **392**, 605–608 (1998).

22. Gasser, T. *et al.* A susceptibility locus for Parkinson's disease maps to chromosome 2p13. *Nat Genet* **18**, 262–265 (1998).

23. Singleton, A. B. Synuclein Locus Triplication Causes Parkinson's Disease. *Science* **302**, 841–841 (2003).

24. Leroy, E. *et al.* The ubiquitin pathway in Parkinson's disease. *Nature* **395**, 451–452 (1998).

25. Valente, E. M. Hereditary Early-Onset Parkinson's Disease Caused by Mutations in PINK1. *Science* **304**, 1158–1160 (2004).

26. Bonifati, V. *et al.* DJ-1 (PARK7), a novel gene for autosomal recessive, early onset parkinsonism. *Neurol Sci* **24**, 159–160 (2003).

27. Paisán-Ruíz, C. *et al.* Cloning of the Gene Containing Mutations that Cause PARK8-Linked Parkinson's Disease. *Neuron* **44**, 595–600 (2004).

28. Ramirez, A. *et al.* Hereditary parkinsonism with dementia is caused by mutations in ATP13A2, encoding a lysosomal type 5 P-type ATPase. *Nat Genet* **38**, 1184–1191 (2006).

29. Hicks, A. A. *et al.* A susceptibility gene for late-onset idiopathic Parkinson's disease: PD Susceptibility Gene. *Ann Neurol.* **52**, 549–555 (2002).

30. Pankratz, N. *et al.* Significant Linkage of Parkinson Disease to Chromosome 2q36-37. *Am J Hum Genet* **72**, 1053–1057 (2003).

31. Pankratz, N. *et al.* Genome-wide linkage analysis and evidence of gene-by-gene interactions in a sample of 362 multiplex Parkinson disease families. *Hum. Mol. Genet.* **12**, 2599–2608 (2003).

32. Strauss, K. M. *et al.* Loss of function mutations in the gene encoding Omi/HtrA2 in Parkinson's disease. *Hum Mol Genet* **14**, 2099–2111 (2005).

33. Paisan-Ruiz, C. *et al.* Characterization of PLA2G6 as a locus for dystonia-parkinsonism. *Ann Neurol.* **65**, 19–23 (2008).

34. Fonzo, A. D. *et al.* FBXO7 mutations cause autosomal recessive, early-onset parkinsonian-pyramidal syndrome. *Neurology* **72**, 240–245 (2009).

35. Satake, W. *et al.* Genome-wide association study identifies common variants at four loci as genetic risk factors for Parkinson's disease. *Nat Genet* **41**, 1303–1307 (2009).

36. Vilariño-Güell, C. *et al.* VPS35 Mutations in Parkinson Disease. *The American Journal of Human Genetics* **89**, 162–167 (2011).

37. Chartier-Harlin, M.-C. *et al.* Translation Initiator EIF4G1 Mutations in Familial Parkinson Disease. *The American Journal of Human Genetics* **89**, 398–406 (2011).

38. Edvardson, S. *et al.* A Deleterious Mutation in DNAJC6 Encoding the Neuronal-Specific Clathrin-Uncoating Co-Chaperone Auxilin, Is Associated with Juvenile Parkinsonism. *PLoS One* **7**, (2012).

39. Krebs, C. E. *et al.* The Sac1 domain of SYNJ1 identified mutated in a family with early-onset progressive parkinsonism with generalized seizures. *Hum Mutat* **34**, 1200–1207 (2013).

40. Quadri, M. *et al.* Mutation in the SYNJ1 Gene Associated with Autosomal Recessive, Early-Onset Parkinsonism. *Human Mutation* **34**, 1208–1215 (2013).

41. Deng, H.-X. *et al.* Identification of TMEM230 mutations in familial Parkinson's disease. *Nat Genet* **48**, 733–739 (2016).

42. Vilariño-Güell, C. *et al.* DNAJC13 mutations in Parkinson disease. *Hum Mol Genet* **23**, 1794–1801 (2014).

43. Funayama, M. *et al.* CHCHD2 mutations in autosomal dominant late-onset Parkinson's disease: a genome-wide linkage and sequencing study. *The Lancet Neurology* **14**, 274–282 (2015).

44. Lesage, S. *et al.* Loss of VPS13C Function in Autosomal-Recessive Parkinsonism Causes Mitochondrial Dysfunction and Increases PINK1/Parkin-Dependent Mitophagy. *The American Journal of Human Genetics* **98**, 500–513 (2016).

45. Sudhaman, S. *et al.* Evidence of mutations in RIC3 acetylcholine receptor chaperone as a novel cause of autosomal-dominant Parkinson's disease with non-motor phenotypes. *J Med Genet* **53**, 559–566 (2016).

46. Matsumine, H. *et al.* Localization of a gene for an autosomal recessive form of juvenile Parkinsonism to chromosome 6q25.2-27. *Am J Hum Genet* **60**, 588–596 (1997).

47. Seirafi, M., Kozlov, G. & Gehring, K. Parkin structure and function. *FEBS J* **282**, 2076–2088 (2015).

48. Ham, S. J. *et al.* Interaction between RING1 (R1) and the Ubiquitin-like (UBL) Domains Is Critical for the Regulation of Parkin Activity. *J Biol Chem* **291**, 1803–1816 (2016).

49. Martinez, A. *et al.* Quantitative proteomic analysis of Parkin substrates in Drosophila neurons. *Mol Neurodegeneration* **12**, 29 (2017).

50. Goldberg, M. S. *et al.* Parkin-deficient Mice Exhibit Nigrostriatal Deficits but Not Loss of Dopaminergic Neurons. *J. Biol. Chem.* **278**, 43628–43635 (2003).

51. Malik, B. R., Godena, V. K. & Whitworth, A. J. VPS35 pathogenic mutations confer no dominant toxicity but partial loss of function in *Drosophila* and genetically interact with *parkin*. *Hum. Mol. Genet.* **24**, 6106–6117 (2015).

52. Truban, D., Hou, X., Caulfield, T. R., Fiesel, F. C. & Springer, W. PINK1, Parkin, and Mitochondrial Quality Control: What can we Learn about Parkinson's Disease Pathobiology? *J Parkinsons Dis* **7**, 13–29 (2017).

53. de Goede, P., Wefers, J., Brombacher, E. C., Schrauwen, P. & Kalsbeek, A. Circadian rhythms in mitochondrial respiration. *J Mol Endocrinol* **60**, R115–R130 (2018).

54. Mitra, K. Mitochondrial fission-fusion as an emerging key regulator of cell proliferation and differentiation. *Bioessays* **35**, 955–964 (2013).

55. Wai, T. & Langer, T. Mitochondrial Dynamics and Metabolic Regulation. *Trends Endocrinol. Metab.* **27**, 105–117 (2016).

56. Ni, H.-M., Williams, J. A. & Ding, W.-X. Mitochondrial dynamics and mitochondrial quality control. *Redox Biol* **4**, 6–13 (2015).

57. Beal, M. F. Aging, energy, and oxidative stress in neurodegenerative diseases. *Ann. Neurol.* **38**, 357–366 (1995).

58. Blesa, J., Trigo-Damas, I., Quiroga-Varela, A. & Jackson-Lewis, V. R. Oxidative stress and Parkinson's disease. *Front Neuroanat* **9**, (2015).

59. Mizuno, Y. *et al.* Deficiencies in complex I subunits of the respiratory chain in Parkinson's disease. *Biochem. Biophys. Res. Commun.* **163**, 1450–1455 (1989).

60. Hristova, V. A., Beasley, S. A., Rylett, R. J. & Shaw, G. S. Identification of a novel Zn2+-binding domain in the autosomal recessive juvenile Parkinson-related E3 ligase parkin. *J. Biol. Chem.* **284**, 14978–14986 (2009).

61. Trempe, J.-F. *et al.* Structure of Parkin Reveals Mechanisms for Ubiquitin Ligase Activation. *Science* **340**, 1451–1455 (2013).

62. Dye, B. T. & Schulman, B. A. Structural mechanisms underlying posttranslational modification by ubiquitin-like proteins. *Annu Rev Biophys Biomol Struct* **36**, 131–150 (2007).

63. Wenzel, D. M., Lissounov, A., Brzovic, P. S. & Klevit, R. E. UBCH7 reactivity profile reveals parkin and HHARI to be RING/HECT hybrids. *Nature* **474**, 105–108 (2011).

64. Sarraf, S. A. *et al.* Landscape of the PARKIN-dependent ubiquitylome in response to mitochondrial depolarization. *Nature* **496**, 372–376 (2013).

65. Fallon, L. *et al.* A regulated interaction with the UIM protein Eps15 implicates parkin in EGF receptor trafficking and PI(3)K-Akt signalling. *Nat. Cell Biol.* **8**, 834–842 (2006).

66. Chaugule, V. K. *et al.* Autoregulation of Parkin activity through its ubiquitin-like domain. *EMBO J.* **30**, 2853–2867 (2011).

67. Koyano, F. *et al.* Ubiquitin is phosphorylated by PINK1 to activate parkin. *Nature* **510**, 162–166 (2014).

68. Kane, L. A. *et al.* PINK1 phosphorylates ubiquitin to activate Parkin E3 ubiquitin ligase activity. *J. Cell Biol.* **205**, 143–153 (2014).

69. Riley, B. E. *et al.* Structure and function of Parkin E3 ubiquitin ligase reveals aspects of RING and HECT ligases. *Nat Commun* **4**, 1982 (2013).

70. Yamano, K. *et al.* Site-specific Interaction Mapping of Phosphorylated Ubiquitin to Uncover Parkin Activation. *J. Biol. Chem.* **290**, 25199–25211 (2015).

71. Lazarou, M. *et al.* The ubiquitin kinase PINK1 recruits autophagy receptors to induce mitophagy. *Nature* **524**, 309–314 (2015).

72. Stolz, A., Ernst, A. & Dikic, I. Cargo recognition and trafficking in selective autophagy. *Nat. Cell Biol.* **16**, 495–501 (2014).

73. Tanaka, A. *et al.* Proteasome and p97 mediate mitophagy and degradation of mitofusins induced by Parkin. *J. Cell Biol.* **191**, 1367–1380 (2010).

74. Vincow, E. S. *et al.* The PINK1-Parkin pathway promotes both mitophagy and selective respiratory chain turnover in vivo. *Proc. Natl. Acad. Sci. U.S.A.* **110**, 6400–6405 (2013).

75. Soubannier, V. *et al.* A vesicular transport pathway shuttles cargo from mitochondria to lysosomes. *Curr. Biol.* **22**, 135–141 (2012).

76. McLelland, G.-L., Soubannier, V., Chen, C. X., McBride, H. M. & Fon, E. A. Parkin and PINK1 function in a vesicular trafficking pathway regulating mitochondrial quality control. *EMBO J.* **33**, 282–295 (2014).

77. Braschi, E. *et al.* Vps35 mediates vesicle transport between the mitochondria and peroxisomes. *Curr. Biol.* **20**, 1310–1315 (2010).

78. Swatek, K. N. & Komander, D. Ubiquitin modifications. *Cell Res.* **26**, 399–422 (2016).

79. Wu, Z. *et al.* Mechanisms controlling mitochondrial biogenesis and respiration through the thermogenic coactivator PGC-1. *Cell* **98**, 115–124 (1999).

80. Johnson, B. N., Berger, A. K., Cortese, G. P. & Lavoie, M. J. The ubiquitin E3 ligase parkin regulates the proapoptotic function of Bax. *Proc. Natl. Acad. Sci. U.S.A.* **109**, 6283–6288 (2012).

81. Borbély, A. A., Daan, S., Wirz-Justice, A. & Deboer, T. The two-process model of sleep regulation: a reappraisal. *J Sleep Res* **25**, 131–143 (2016).

82. Reinke, H. & Asher, G. Crosstalk between metabolism and circadian clocks. *Nat Rev Mol Cell Biol* **20**, 227–241 (2019).

83. Hatori, M. & Panda, S. The emerging roles of melanopsin in behavioral adaptation to light. *Trends Mol Med* **16**, 435–446 (2010).

84. Buijs, F. N. *et al.* The Circadian System: A Regulatory Feedback Network of Periphery and Brain. *Physiology (Bethesda)* **31**, 170–181 (2016).

85. Neufeld-Cohen, A. *et al.* Circadian control of oscillations in mitochondrial rate-limiting enzymes and nutrient utilization by PERIOD proteins. *Proc. Natl. Acad. Sci. U.S.A.* **113**, E1673-1682 (2016).

86. Peek, C. B. *et al.* Circadian clock NAD+ cycle drives mitochondrial oxidative metabolism in mice. *Science* **342**, 1243417 (2013).

87. Jacobi, D. *et al.* Hepatic Bmal1 Regulates Rhythmic Mitochondrial Dynamics and Promotes Metabolic Fitness. *Cell Metab.* **22**, 709–720 (2015).

88. Schmitt, K. *et al.* Circadian Control of DRP1 Activity Regulates Mitochondrial Dynamics and Bioenergetics. *Cell Metabolism* **27**, 657-666.e5 (2018).

89. Li, S., Wang, Y., Wang, F., Hu, L.-F. & Liu, C.-F. A New Perspective for Parkinson's Disease: Circadian Rhythm. *Neurosci. Bull.* **33**, 62–72 (2017).

90. Kawarai, T., Kawakami, H., Yamamura, Y. & Nakamura, S. Structure and organization of the gene encoding human dopamine transporter. *Gene* **195**, 11–18 (1997).

91. Mukherjee, S. *et al.* Knockdown of Clock in the ventral tegmental area through RNA interference results in a mixed state of mania and depression-like behavior. *Biol. Psychiatry* **68**, 503–511 (2010).

92. Yujnovsky, I., Hirayama, J., Doi, M., Borrelli, E. & Sassone-Corsi, P. Signaling mediated by the dopamine D2 receptor potentiates circadian regulation by CLOCK:BMAL1. *Proc. Natl. Acad. Sci. U.S.A.* **103**, 6386–6391 (2006).

93. Pacelli, C. *et al.* Parkin Mutation Affects Clock Gene-Dependent Energy Metabolism. *Int J Mol Sci* **20**, (2019).

94. Rosati, J. *et al.* Establishment of stable iPS-derived human neural stem cell lines suitable for cell therapies. *Cell Death Dis* **9**, 937 (2018).

95. Cornelissen, G. Cosinor-based rhythmometry. *Theor Biol Med Model* **11**, 16 (2014).

96. Agriesti, F., Cela, O. & Capitanio, N. “Time Is out of Joint” in Pluripotent Stem Cells: How and Why. *Int J Mol Sci* **25**, 2063 (2024).

97. Partch, C. L., Green, C. B. & Takahashi, J. S. Molecular Architecture of the Mammalian Circadian Clock. *Trends Cell Biol* **24**, 90–99 (2014).

98. Videnovic, A. & Golombek, D. Circadian dysregulation in Parkinson’s disease. *Neurobiol Sleep Circadian Rhythms* **2**, 53–58 (2016).

99. Jin, S. M. & Youle, R. J. PINK1- and Parkin-mediated mitophagy at a glance. *J Cell Sci* **125**, 795–799 (2012).

100. Shaltouki, A. *et al.* Mitochondrial Alterations by PARKIN in Dopaminergic Neurons Using PARK2 Patient-Specific and PARK2 Knockout Isogenic iPSC Lines. *Stem Cell Reports* **4**, 847–859 (2015).